



# HHS Public Access

Author manuscript

*J Med Chem.* Author manuscript; available in PMC 2020 August 13.

Published in final edited form as:

*J Med Chem.* 2020 May 14; 63(9): 4867–4879. doi:10.1021/acs.jmedchem.0c00202.

## Structure-Based Design of Highly Potent HIV-1 Protease Inhibitors Containing New Tricyclic Ring P2-Ligands: Design, Synthesis, Biological, and X-ray Structural Studies

**Arun K. Ghosh,**

Department of Chemistry, Department of Medicinal Chemistry and Molecular Pharmacology, Purdue University, West Lafayette, Indiana 47907, United States

**Satish Kovala,**

Department of Chemistry, Department of Medicinal Chemistry and Molecular Pharmacology, Purdue University, West Lafayette, Indiana 47907, United States

**Heather L. Osswald,**

Department of Chemistry, Department of Medicinal Chemistry and Molecular Pharmacology, Purdue University, West Lafayette, Indiana 47907, United States

**Masayuki Amano,**

Departments of Infectious Diseases and Hematology, Kumamoto University Graduate School of Biomedical Sciences, Kumamoto 860-8556, Japan

**Manabu Aoki,**

Department of Medical Technology, Kumamoto Health Science University, Kumamoto 861-5598, Japan; Experimental Retrovirology Section, HIV and AIDS Malignancy Branch, National Cancer Institute, National Institutes of Health, Bethesda, Maryland 20892, United States; Department of Clinical Sciences, Kumamoto University Hospital, Kumamoto 860-8556, Japan

**Johnson Agniswamy,**

Department of Biology, Georgia State University, Atlanta, Georgia 30303, United States

**Yuan-Fang Wang,**

Department of Biology, Georgia State University, Atlanta, Georgia 30303, United States

**Irene T. Weber,**

Department of Biology, Georgia State University, Atlanta, Georgia 30303, United States

**Hiroaki Mitsuya**

Department of Refractory Viral Infection, National Center for Global Health and Medicine Research Institute, Tokyo 162-8655, Japan; Experimental Retrovirology Section, HIV and AIDS

---

**Corresponding Author** Phone: (765)-494-5323; akghosh@purdue.edu; Fax: (765)-496-1612.

Supporting Information

The Supporting Information is available free of charge at <https://pubs.acs.org/doi/10.1021/acs.jmedchem.0c00202>.

Molecular formula strings and some data (CSV)

Full NMR spectroscopic data for all final compounds X-ray structural data for inhibitors **4a** and **5c**-bound HIV-1 Protease (PDF)

Accession Codes

The PDB accession codes for X-ray structures of inhibitor **4a** and **5c**-bound HIV-1 protease are: 6VOD and 6VOE.

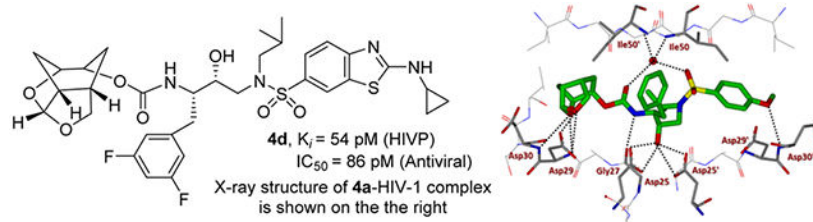
The authors declare no competing financial interest.

Malignancy Branch, National Cancer Institute, National Institutes of Health, Bethesda, Maryland 20892, United States; Department of Clinical Sciences, Kumamoto University Hospital, Kumamoto 860-8556, Japan

## Abstract

We describe here design, synthesis, and biological evaluation of a series of highly potent HIV-1 protease inhibitors containing stereochemically defined and unprecedented tricyclic furanofuran derivatives as P2 ligands in combination with a variety of sulfonamide derivatives as P2' ligands. These inhibitors were designed to enhance the ligand-backbone binding and van der Waals interactions in the protease active site. A number of inhibitors containing the new P2 ligand, an aminobenzothiazole as the P2' ligand and a difluorophenylmethyl as the P1 ligand, displayed very potent enzyme inhibitory potency and also showed excellent antiviral activity against a panel of highly multidrug-resistant HIV-1 variants. The tricyclic P2 ligand has been synthesized efficiently in an optically active form using enzymatic desymmetrization of meso-1,2-(dihydroxymethyl)cyclohex-4-ene as the key step. We determined high-resolution X-ray structures of inhibitor-bound HIV-1 protease. These structures revealed extensive interactions with the backbone atoms of HIV-1 protease and provided molecular insights into the binding properties of these new inhibitors.

## Graphical Abstract



## INTRODUCTION

HIV-1 protease inhibitors (PIs) are critical components of combined antiretroviral therapy (cART) which dramatically improved the HIV-related mortality and morbidity to patients with HIV-1 infection and AIDS.<sup>1,2</sup> PIs block the cleavage of Gag-Pol polyproteins during viral maturation and result in generation of noninfectious virions.<sup>3,4</sup> PI-based drugs in general exhibit a relatively high genetic barrier to the emergence of drug-resistant HIV-1 variants compared to non-nucleoside reverse transcriptase inhibitors and integrase strand transfer inhibitors (INSTIs).<sup>5-7</sup> The last approved PI, darunavir (**1**, DRV, Figure 1), is a first-line therapy which is often preferred for cART-naïve HIV-1 infected patients because of its tolerance and a high genetic barrier to the development of drug-resistant viruses.<sup>8-10</sup> However, there are reports of failure of DRV-containing regimens and the emergence of darunavir resistant HIV-1 variants.<sup>11,12</sup> Furthermore, there are reports that a growing number of HIV/AIDS patients are harboring highly multidrug-resistant HIV-1 variants, and options for treating these patients are limited.<sup>13,14</sup> Therefore, the development of potent and structurally novel PIs with broad spectrum antiviral activity are necessary for the future success of cART treatment regimens.

Darunavir and its derivatives (**2**) were designed to promote a network of hydrogen bonding interactions with the backbone atoms at the active site of HIV-1 protease. The backbone binding strategies are likely to slow development of drug resistant HIV-1 variants because of possible reduction of catalytic fitness. Darunavir incorporated the stereochemically defined and conformationally constrained bicyclic polyether, *bis*-tetrahydrofuran (*bis*-THF), which makes extensive interactions in the active site.<sup>10,15,16</sup> Numerous X-ray crystallographic studies of darunavir-bound HIV-1 protease revealed that darunavir forms a network of hydrogen bonding interactions with the backbone of HIV-1 protease in both S2 and S2' subsites.<sup>17,18</sup> The P2 *bis*-tetrahydrofuranyl urethane (*bis*-THF) ligand is an intriguing pharmacophore where both ring oxygens form strong hydrogen bonds with the Asp29 and Asp30 backbone amide NHs. The bicyclic *bis*-THF ring also engages in van der Waals interaction with active site residues.<sup>19,20</sup> In our continuing efforts to optimize both P2 and P2' structural templates of darunavir, we have recently reported a number of very potent PIs with unprecedented structural features.<sup>21-23</sup> In particular, we designed a crown-like tetrahydropyrano-tetrahydrofuran in inhibitor **3** with a bridged methylene group as the P2 ligand to promote additional van der Waals interactions in the active site.<sup>24,25</sup> Inhibitors containing such *crown*-THF ligands are very potent inhibitors and maintained potent antiviral activity against multidrug-resistant HIV-1 variants.<sup>25,26</sup> The X-ray structural analysis of *crown*-THF-derived inhibitors provided molecular insights to further improve ligand-binding site interactions.<sup>24,25</sup> Herein, we report a new class of PIs containing cyclohexane fused *bis*-tetrahydrofuran as the P2 ligands in combination with (*R*)-hydroxyethylaminesulfonamide isosteres. A number of inhibitors exhibited exceptionally potent enzyme inhibitory and antiviral activity. In particular, inhibitor **4d** maintained exceptional antiviral potency against selected multidrug-resistant HIV-1 variants. Our high resolution X-ray structural studies of inhibitor-bound HIV-1 protease revealed important molecular insights into the ligand-binding site interactions responsible for their potent activity. The design and synthesis of new PIs have been an active area of our research. Several potent inhibitors incorporating a variety of heterocyclic P2 ligands for improving interactions at the S2 subsite have been reported.<sup>27-30</sup> A number of other design efforts were focused on optimizing both P1 and P2' moieties to improve potency.<sup>27,28,31</sup> Recently, bicyclic piperazine sulfonamide-based inhibitors have been designed where the piperazine NH forms the key interaction with the catalytic aspartic acids of the HIV-1 protease.<sup>32,33</sup>

## RESULTS AND DISCUSSION

Based upon ligand-binding site interactions of the *crown*-THF ligand in **3** in the HIV-1 protease active site, we have designed a new tricyclic cyclohexane fused-tetrahydrofuranofuran (*Chf*-THF) derivative as the P2 ligand shown in inhibitors **4a** and **5a** (Table 1). This new design may promote better hydrogen bonding interactions with backbone atoms. Furthermore, the new ligand with additional methylene groups around the *bis*-THF may exhibit better van der Waals interactions in the active site. Our preliminary model of the enantiomeric ligand structure also showed good orientation for hydrogen bonding interactions with backbone amide NHs of Asp29 and Asp30. The conformationally constrained ligand also appeared to engage in additional van der Waals contacts in the S2 subsite compared to the *bis*-THF ligand to darunavir. While the stereochemistry of the *Chf*-

ligand in inhibitors **4a** and **5a** appeared optimum, we planned to synthesize both enantiomeric ligands as both enantiomers of *bis*-THF ligand and *crown*-THF in inhibitor **3** showed comparable enzyme affinity and ligand binding site interactions. This is due to the fact that the acetal oxygens in both enantiomers are in a similar environment and both ligands can form strong hydrogen bonds with the backbone amide residues in the S2 subsite. Therefore, our plan is to synthesize both enantiomers and gain molecular insights into their ligand-binding site interactions using X-ray structural studies of the inhibitor-HIV-1 protease complex. We also plan to examine various hydroxyethylsulfonamide isosteres containing varying P1 and P2' ligands. In particular, we plan to investigate an aminobenzothiazole(Abt)-based P2'-ligand which has been showed to promote better hydrogen bonding and van der Waals interactions compared to the 4-aminobenzene-sulfonamide P2'-ligand of darunavir. Structurally, the Abt P2' ligand forms additional hydrogen bonding and van der Waals interactions in the S2' subsite. A number of recent inhibitors containing these P2'-ligands exhibited robust antiviral activity against highly multidrug-resistant HIV-1 variants.<sup>24,25</sup>

For our studies, we plan to synthesize our newly designed ligand in a stereodefined manner. Our synthetic strategy for optically active synthesis is shown in Scheme 1. Enantiomeric ligand **6** can be obtained from the functionalized cyclohexane-1,2-diol derivative **7**. Structure **7** can be obtained from cyclohexene derivative **8** by asymmetric dihydroxylation reaction.<sup>34,35</sup> An optically active aldehyde derivative can be derived conveniently from meso diol derivative **9** by enzymatic desymmetrization as the key reaction. The meso-diol **9** can be derived from commercially available and inexpensive 1,2,3,6-tetrahydrophthalic anhydride **10**.

Our synthesis of optically active ligand **6** is shown in Scheme 2. *meso*-1,2,3,6-Tetrahydrophthalic anhydride **10** was reduced by LiAlH<sub>4</sub> in THF at 0 °C for 3 h to provide meso-diol derivative **9** in a multigram scale.<sup>36</sup> Diol **9** was subjected to enzymatic desymmetrization reaction using porcine pancreatic lipase (PPL) in ethyl acetate at 23 °C for 12 h to provide monoacetate derivative **11** in gram scale in 82% yield and >95% ee, as determined by high-performance liquid chromatography (HPLC) analysis<sup>37</sup> (see Supporting Information for further details). Swern oxidation of alcohol **11** provided the corresponding aldehyde which was reacted with trimethylorthoformate in the presence of a catalytic amount of tetrabutylammonium tribromide (TBABr<sub>3</sub>) at 23 °C for 8 h to provide dimethylacetal derivative **12** in 76% yield over two steps. For diastereoselective dihydroxylation, we carried out Sharpless asymmetric dihydroxylation using AD-mix- $\beta$ .<sup>34</sup> Reaction of **12** with AD-mix- $\beta$  in a mixture (1:1) of *t*-butanol and water at 0–23 °C for 24 h resulted in a 1:1 mixture of diastereomeric diol.<sup>38</sup> The resulting diol was subjected to saponification using 1 N aqueous NaOH in MeOH at 0–23 °C for 3 h to provide triol derivatives **13** and **14** in 90% yield over two steps. These triol derivatives were separated by silica gel chromatography using 5% MeOH in CH<sub>2</sub>Cl<sub>2</sub> as the eluent. Triol derivative **13** was reacted with a catalytic amount of camphorsulfonic acid (CSA) in CH<sub>2</sub>Cl<sub>2</sub> at 0 °C for 1 h to provide optically active tricyclic ligand alcohol **6** in 82% yield.

Our synthesis of enantiomeric ligand *ent*-**6** from *meso*-diol **9** is shown in Scheme 2. Diol **9** was converted to diacetate derivative **15** by reaction with acetic anhydride and pyridine in

the presence of a catalytic amount of DMAP at 23 °C for 16 h. Exposure of diacetate to PPL in 0.1 M phosphate buffer at pH 7 in the presence of aqueous NaHCO<sub>3</sub> at 23 °C for 16 h provided optically active alcohol *ent*-**11** in 84% yield.<sup>37,39</sup> Alcohol *ent*-**11** was converted to dimethylacetal *ent*-**12** in 80% yield as described above. Exposure of dimethylacetal *ent*-**12** to sharpless asymmetric dihydroxylation reaction with AD-mix-*α* afforded a 1:1 mixture of diastereomeric diol.<sup>34</sup> Deprotection of the acetate derivative furnished triol derivatives *ent*-**13** and *ent*-**14** which were separated by silica gel chromatography. Treatment of the major triol derivative *ent*-**13** with a catalytic amount of CSA in CH<sub>2</sub>Cl<sub>2</sub> afforded ligand alcohol *ent*-**6** in 79% yield.

The synthesis of the designed PIs was carried out in a two-step sequence involving synthesis of activated carbonates followed by reaction of these carbonates with appropriate hydroxyethylaminesulfonamide isosteres.<sup>22,23</sup> The syntheses of various activated carbonates are shown in Scheme 3. Optically active ligand alcohols **6** and *ent*-**6** synthesized above were converted to their respective activated carbonates **16** and *ent*-**16**. As shown, reaction of ligand alcohols **6** and *ent*-**6** with 4-nitrophenylchloroformate in the presence of pyridine in CH<sub>2</sub>Cl<sub>2</sub> at 0–23 °C for 12 h provided activated carbonates **16** and *ent*-**16** in 87 and 88% yields, respectively. These carbonates were then converted to urethane derivatives using amines **17–22**. The synthesis of various inhibitors containing *Chf*-THF as the P2 ligands on the hydroxyethylamine sulfonamide isostere is shown in Scheme 4. Reactions of activated carbonate **16** with known<sup>22,23</sup> amine derivatives **17–22** in the presence of diisopropylethylamine (DIPEA) in CH<sub>3</sub>CN at 23 °C for 72 h provided inhibitors **4a–f** in good yields (65–86%). Similarly, reactions of carbonate *ent*-**16** with amines **17–22** under similar conditions afforded inhibitors **5a–5f** in very good yields (59–87%). The full structures of these inhibitors are shown in Table 1.

Our preliminary model of the P2 *Chf*-THF ligand in inhibitor **4a** compared to the *bis*-THF ligand in inhibitor **2** indicated that both oxygens of the new *Chf*-THF ligand could align optimally with Asp29 and Asp30 backbone amide NHs in the S2 site. In addition, two methylene groups are expected to provide van der Waals interactions surrounding Ile47, Val32, Leu76, and Ile50' residues in the S2 subsite. Because ligand combinations are critical for overall affinity, we investigated enantiomeric *Chf*-THF with various P2'-ligands. The results of compounds in HIV-1 protease inhibitory and antiviral assays are shown in Table 1. The assay protocol for HIV-1 inhibition is similar to the reported procedure of Toth and Marshall.<sup>40</sup> The protocol for antiviral assay is described previously using MT-2 human T-lymphoid cells exposed to HIV-1<sub>LAI</sub>.<sup>40</sup> To assess the stereochemical effect, we first examined the enantiomeric ligands in combination with a sulfonamide isostere with a 4-methoxy benzene sulfonamide as the P2'-ligand in compounds **4a** and **5a**. Inhibitor **4a** showed very potent HIV-1 protease inhibitory activity with a *K<sub>i</sub>* value of 8 pM. The inhibitor **4a** also exhibited a very good antiviral IC<sub>50</sub> value of 38 nM (entry 1). Inhibitor **5a** with enantiomeric *Chf*-THF ligand is slightly less potent than **4a**. It showed enzyme inhibitory activity with a *K<sub>i</sub>* of 34 pM and antiviral activity with an IC<sub>50</sub> value of 72 nM (entry 2). We then examined both enantiomeric ligands in combination with other benzothiazoles and benzoxazoles as the P2'-ligands. Inhibitor **4b** showed very potent enzyme *K<sub>i</sub>* of 2 pM, which is nearly 10-fold better than inhibitor **5b** with the enantiomeric P2 ligand (entries 3 and 4).

However, both inhibitors exhibited very potent antiviral activity with  $IC_{50}$  values of 3.3 and 1.8 nM. Inhibitors **4c** and **5c** with enantiomeric *Chf*-THF P2 ligands and benzoxazole P2' ligands also showed very potent enzyme inhibitors and antiviral activity (entries 5 and 6). Interestingly, inhibitor **5c** exhibited over 5-fold improvement of antiviral activity ( $IC_{50} = 0.3$  nM) compared to inhibitor **4c** ( $IC_{50} = 1.7$  nM).

We then examined inhibitors containing enantiomeric *Chf*-THF ligands in combination with fluorine-substituted phenylmethyl groups as the P1 ligands. As shown in Table 2, incorporation of a 3,5-difluoro phenylmethyl group as the P1-ligand resulted in inhibitor **4d** which displayed enzyme inhibitory  $K_i$  of 54 pM and antiviral  $IC_{50}$  value of 86 pM. Inhibitor **4d** showed improved antiviral activity compared to the corresponding inhibitor **4b** containing a phenylmethyl group as the P1-ligand. This improvement in antiviral activity may be due to increased lipophilicity of inhibitor **4d** (clogP 5.4) over inhibitor **4b** (clogP 5.1). Inhibitor **5d** containing the enantiomeric P2 ligand also showed very potent enzyme  $K_i$  value; however, it showed nearly 25-fold reduction of antiviral activity compared to inhibitor **4d** with an enantiomeric P2 ligand (entries 1 and 2). In comparison, darunavir and saquinavir exhibited antiviral  $IC_{50}$  values of 3.2 and 21 nM, respectively. We also examined the effect of monofluoro substitution on the P1-ligand. As shown, incorporation of 3-fluorophenylmethyl as the P1 ligand resulted in inhibitors **4e** and **5e** with only marginal improvement of antiviral activity compared to unsubstituted P1 ligands in inhibitors **4b** and **5b** (Table 1). Incorporation of 4-fluoro phenylmethyl as the P1 ligand resulted in inhibitors **4f** and **5f** with improvement of antiviral activity, over 7-fold compared to inhibitor **4b** and over 4-fold compared to inhibitor **5b** (entry 3, Table 1). Overall, inhibitor **4d** with 3,5-*bis*-fluorines on the P1 ligand showed the best antiviral activity over methoxy sulfonamide and monofluoro derivatives.

While the cART therapy and treatment guidelines are updated regularly, PI-based drugs are important elements of current cART regimens. In particular, PIs are widely used for the treatment of naïve and experienced HIV/AIDS patients. As mentioned earlier, heavily-ART regimen-experienced HIV/AIDS patients are reported to have drug-failure with the currently available PIs including DRV.<sup>11,12</sup> Therefore, the design of new classes of potent PIs with a high genetic barrier to development of drug resistance is important for durable treatment options. In this context, our long-standing objective is to design PIs that can maintain robust potency against a variety of existing multi-PI-resistant HIV-1 variants with better selectivity index and safety profiles. Based upon preliminary antiviral data, we selected two potent inhibitors (**4d**, antiviral  $IC_{50}$  of 0.086 nM and **5c**, antiviral  $IC_{50}$  of 0.3 nM) containing enantiomeric *Chf*-THF ligands and evaluated their antiviral activity against a panel of highly multidrug-resistant HIV-1 variants that had been selected *in vitro* with widely used FDA-approved PIs, ATV and DRV. Each of these HIV-1 variants were selected *in vitro* by propagating HIV-1<sub>NL4-3</sub> in the presence of increasing concentrations of each PI (up to 5  $\mu$ M) in MT-4 cells, as described by us previously.<sup>41,42</sup> The results are shown in Table 3. As can be seen, both widely used PI drugs, ATV and DRV, lost activity against these resistant variants. In particular, ATV lost significant potency and is unable to suppress the replication of highly PI-resistant HIV-1 variants examined. DRV showed relatively better results compared to ATV; however, DRV lost 86-fold and 89-fold activity against HIV-1<sub>LPV-5</sub>  $\mu$ M



and HIV-1<sub>DRV</sub><sup>R</sup><sub>P30</sub> variants. Inhibitor **5c** containing the *Chf*-THF P2 ligand failed to block replication of these highly drug-resistant HIV-1 variants. Inhibitor **4d** containing enantiomeric P2-ligand is significantly more potent than DRV and ATV against HIV-1<sub>NL4-3</sub> virus. While this inhibitor maintained very good antiviral activity (0.21–4.5 nM) against these highly drug-resistant HIV-1 variants, its fold-change of activity is comparable to DRV. The reason for better overall antiviral activity is possibly due to extensive hydrogen bonding and van der Waals interactions in the S2 and S2' subsites. Our X-ray crystallographic studies of inhibitors **4a**- and **5c**-bound HIV-1 protease provided molecular insights into the ligand-binding site interactions responsible for their activity.

We determined the X-ray structures of inhibitors **4a** and **5c** containing enantiomeric ligands in complex with wild-type HIV-1 protease at a resolution of 1.25 and 1.3 Å, respectively.<sup>43</sup> Both complexes crystallized in the orthorhombic space group *P2*<sub>1</sub>*2*<sub>1</sub>*2* with one protease homodimer per asymmetric unit. The inhibitors bind at the active site in two alternate conformations related by 180° rotation with a relative occupancy of 0.7/0.3 for inhibitor **4a** and 0.55/0.45 for inhibitor **5c**. The overall dimer structure is very similar to the HIV-1 protease–darunavir complex<sup>17,18</sup> with an rmsd for superposition of 198 equivalent *C $\alpha$*  atoms of 0.14 Å and 0.12 for protease complexes with inhibitors **4a** and **5c**, respectively. The largest deviation of 0.45 Å in comparison to the protease–darunavir complex occurs at residue Pro39 for **5c** complex, while flap residue Phe53' exhibits a maximum deviation of 0.51 Å in **4a** complex. The key interactions of inhibitors **4a** and **5c** with HIV-1 protease are highlighted in Figures 2 and 3, respectively. Both inhibitors retain all the hydrogen bonds observed between darunavir and the main chain atoms of the HIV-1 protease. The new inhibitors also form a tetracoordinated water-mediated hydrogen bond interaction involving one of the sulfonamide oxygens and carbonyl oxygen with the amide nitrogen of flap residues Ile 50 and Ile 50' similar to the protease–darunavir complex.<sup>44</sup>

Inhibitor **5c** has a *Chf*-THF as P2 group and the two acetal oxygens in the bulky *Chf*-THF form hydrogen bond interactions with the main chain amide of Asp29 and Asp30 similar to the hydrogen bonds formed by the *bis*-THF oxygens in darunavir. However, unlike the *bis*-THF of darunavir, the bigger *Chf*-THF of inhibitors **4a** and **5c** form a number of additional van der Waals interactions. We compared van der Waals interactions of the enantiomeric *Chf*-THF ligands in Figure 4. Interestingly, in one conformation, *Chf*-ligand in compound **5c** forms van der Waals contacts with Ile47. The tricyclic core of the *Chf*-THF ligand forms van der Waals interaction with the side chain atoms of Ile47, the main chain amide of Gly48, and the C $\delta$ 1 atom of Ile50'. The two acetal oxygens in the enantiomeric P2 *Chf*-THF of **4a** are shifted by 0.8 Å in comparison to those of **5c**. There is an additional hydrogen bond interaction between one of the acetal oxygens and the carboxylate side chain of Asp29. Further, the enantiomeric change allows the 6-member ring of *Chf*-THF in inhibitor **4a** to shift toward Ile84. Because of this shift, the P2 group of **4a** form van der Waals interactions with Ile 84 in addition to those with Ile47, Gly48, and Ile50'.

The aminobenzene group at the P2' of darunavir is replaced by the extended *N*-isopropylbenzo[*d*]oxazol-2-amine group in inhibitor **5c**. In the protease–darunavir complex, the P2' amine of darunavir forms direct and water-mediated hydrogen bonds with the two alternate conformations of Asp30' side chain. In the protease complex with **5c**, the single

conformation of Asp30' forms a direct hydrogen bond interaction with the oxazole nitrogen of the inhibitor. In addition, the extended P2' amine group of inhibitor **5c** forms a new hydrogen bond with the carboxylate side chain of Asp30'. Further, the terminal P2' isopropyl group of **5c** forms a C–H...O interaction (2.8–3.2 Å) with the carboxylate side chain of Asp29' and van der Waals interaction with Ile47'. Asp29' plays a vital role in the structural integrity of the protease dimer by forming a conserved inter-subunit ion pair with Arg8. The P2' methoxy group of inhibitor **4a** has a similar position as the P2' aminobenzene of darunavir in the S2' subsite of protease. The oxygen atom of the P2' methoxy group in inhibitor **4a** forms a hydrogen bond with the main chain amide of Asp30'. The *Chf*-THF P2'-ligand in inhibitor **4a** appeared to form enhanced ligand-binding site interactions over the enantiomeric ligand in inhibitor **5c** in the HIV-1 protease active site. The combination of the *Chf*-THF P2'-ligand, 3,5-difluorinated P1 ligand and the aminobenzothiazole P2' ligand resulted in inhibitor **4d** which exhibited best antiviral activity and maintained very good antiviral activity against a panel of highly drug-resistant HIV-1 variants.

## CONCLUSIONS

In summary, based on X-ray structural data, we have designed a new class of very potent HIV-1 PIs incorporating new polycyclic cyclohexane-fused *bis*-tetrahydrofuran derivatives as the P2 ligands. The new ligands have been specifically designed to make favorable hydrogen bonding interactions and van der Waals interactions with the residues at the S2'-subsite. In general, inhibitors containing enantiomeric ligands have shown very potent activity, particularly inhibitors **4d** and **5c**. However, inhibitor **4d** with a difluoro phenylmethyl P1 ligand and an aminobenzothiazole as the P2' ligand maintained very potent activity against a panel of highly multidrug-resistant HIV-1 variants. The results show that inhibitor **4d** is superior to darunavir and other approved PI drugs. The new polycyclic ligand alcohols were synthesized efficiently in an enantioselective manner using enzymatic desymmetrization of *meso*-diols as the key steps. Because both enantiomeric ligands exhibited very high enzyme affinity, we determined high resolution X-ray structures of inhibitor-bound HIV-1 protease containing enantiomeric ligands. As it turned out, both oxygens of the enantiomeric tricyclic ligands formed very strong hydrogen bonds with the backbone amide NHs of Asp29 and Asp30 in the S2 subsite. The P2 ligand in inhibitor **4a** appears to make better van der Waals interactions compared to the enantiomeric ligands in the S2 site. Incorporation of the *Chf*-THF P2 ligand, the fluorinated P1 ligand, and the aminobenzothiazole P2' ligand resulted in inhibitor **4d** that showed best antiviral activity. Further optimization of inhibitor properties and ligand-binding site interactions are in progress in our laboratory.

## EXPERIMENTAL SECTION

### General Methods.

All chemicals and reagents were purchased from commercial suppliers and used without further purification unless otherwise noted. The following reaction solvents were distilled prior to use: dichloromethane from calcium hydride, diethyl ether and tetrahydrofuran from Na/benzophenone, and methanol and ethanol from activated magnesium under argon. All



reactions were carried out under an argon atmosphere in either flame or oven-dried (120 °C) glassware. TLC analysis was conducted using glass-backed thin-layer silica gel chromatography plates (60 Å, 250 μm thickness, F-254 indicator). Column chromatography was performed using 230–400 mesh, 60 Å pore diameter silica gel. <sup>1</sup>H and <sup>13</sup>C NMR spectra were recorded at room temperature on a Bruker AV800, DRX-500 and AV-400. Chemical shifts (δ values) are reported in parts per million and are referenced to the deuterated residual solvent peak. NMR data are reported as δ value (chemical shift, *J*-value (Hz), integration, where s = singlet, d = doublet, t = triplet, q = quartet, and brs = broad singlet). Optical rotations were recorded on a PerkinElmer 341 polarimeter. HRMS and LRMS spectra were recorded at the Purdue University Department of Chemistry Mass Spectrometry Center. HPLC analysis and purification were done on an Agilent 1100 series instrument using a Chiralcel OZ-3 column of 4.6 mm ID for analysis. The purity of all test compounds was determined by HPLC analysis to be 95% pure.

**(1*R*,3*aS*,7*aR*)-Octahydro-1,6-epoxyisobenzofuran-5-yl((2*S*,3*R*)-3-Hydroxy-4-((*N*-isobutyl-4-methoxyphenyl)-sulfonamido)-1-phenylbutan-2-yl)carbamate (4a).**

To a stirred solution of activated alcohol **16** (15 mg, 0.046 mmol) and isostere **17** (21 mg, 0.051 mmol) in acetonitrile (2 mL) was added DIPEA (40 μL, 0.233 mmol) at 23 °C under an argon atmosphere. The reaction mixture was stirred at 23 °C until completion. Upon completion, solvents were removed under reduced pressure and the crude product was purified by silica gel column chromatography (50% EtOAc in hexane) to give **4a** (22 mg, 81%) as an amorphous solid. *R*<sub>f</sub> = 0.3 (70% EtOAc/hexanes). <sup>1</sup>H NMR (500 MHz, CDCl<sub>3</sub>): δ 7.72 (d, *J* = 8.9 Hz, 2H), 7.30–7.23 (m, 4H), 7.22–7.17 (m, 1H), 6.97 (d, *J* = 8.9 Hz, 1H), 5.60 (d, *J* = 3.6 Hz, 1H), 5.02 (d, *J* = 9.3 Hz, 1H), 4.71 (t, *J* = 6.2 Hz, 1H), 4.31 (t, *J* = 5.4 Hz, 1H), 4.10 (m, 1H), 3.87 (m, 1H), 3.86 (s, 3H), 3.82–3.71 (m, 3H), 3.19–3.04 (m, 3H), 2.97 (dd, *J* = 13.4, 8.3 Hz, 1H), 2.83–2.75 (m, 2H), 2.72 (dt, *J* = 8.7, 3.9 Hz, 1H), 2.50 (m, 1H), 1.96 (ddd, *J* = 12.5, 6.0, 4.2 Hz, 1H), 1.91–1.79 (m, 3H), 1.70 (d, *J* = 12.5 Hz, 1H), 1.28 (m, 1H), 0.91 (d, *J* = 6.6 Hz, 3H), 0.86 (d, *J* = 6.6 Hz, 3H); <sup>13</sup>C NMR (125 MHz, CDCl<sub>3</sub>): δ 162.8, 155.8, 137.7, 129.9, 129.4, 129.4, 128.3, 126.3, 114.2, 108.7, 76.2, 75.3, 72.4, 58.6, 55.5, 55.1, 53.5, 42.4, 36.0, 34.1, 29.3, 29.0, 27.1, 20.0, 19.8 LRMS-ESI (*m/z*): 589.2 [M + H]<sup>+</sup>; HRMS-ESI (*m/z*): [M + H]<sup>+</sup> calcd for C<sub>30</sub>H<sub>41</sub>N<sub>2</sub>O<sub>8</sub>S, 589.2578; found, 589.2572.

**(1*R*,3*aS*,7*aR*)-Octahydro-1,6-epoxyisobenzofuran-5-yl((2*S*,3*R*)-4-((2-(Cyclopropylamino)-*N*-isobutylbenzo[*d*]thiazole)-6-sulfonamido)-3-hydroxy-1-phenylbutan-2-yl)carbamate (4b).**

Activated alcohol **16** (8 mg, 0.024 mmol) was treated with isostere amine **18** (14 mg, 0.027 mmol) by following the procedure outlined for inhibitor **4a** to give inhibitor **4b** (12.5 mg, 75%) as an amorphous solid. *R*<sub>f</sub> = 0.15 (80% EtOAc/hexanes). <sup>1</sup>H NMR (500 MHz, CDCl<sub>3</sub>): δ 8.09 (s, 1H), 7.69 (d, *J* = 8.6 Hz, 1H), 7.55 (d, *J* = 8.5 Hz, 1H), 7.39–7.15 (m, 5H), 5.59 (d, *J* = 3.6 Hz, 1H), 5.09 (d, *J* = 9.7 Hz, 1H), 4.70 (m, 1H), 4.31 (t, *J* = 5.5 Hz, 1H), 4.09 (t, *J* = 8.2 Hz, 1H), 3.94–3.71 (m, 4H), 3.21 (dd, *J* = 15.1, 8.9 Hz, 1H), 3.16–3.07 (m, 2H), 3.02 (dd, *J* = 13.4, 8.5 Hz, 1H), 2.86–2.68 (m, 4H), 2.50 (m, 1H), 1.99–1.80 (m, 4H), 1.69 (d, *J* = 12.6 Hz, 1H), 1.26 (m, 1H), 0.97–0.90 (m, 5H), 0.87 (d, *J* = 6.5 Hz, 3H), 0.81–0.77 (m, 2H); <sup>13</sup>C NMR (125 MHz, CDCl<sub>3</sub>): δ 172.9, 155.8, 155.5, 137.7, 131.1, 130.4, 129.4, 128.3, 126.3, 125.3, 120.8, 118.4, 108.7, 76.2, 75.3, 72.4, 58.7, 55.1, 53.6, 42.4, 36.0, 34.0, 29.6,

29.3, 29.0, 27.2, 26.5, 20.1, 19.8, 7.9. LRMS-ESI ( $m/z$ ): 671.2  $[M + H]^+$ ; HRMS-ESI ( $m/z$ ):  $[M + H]^+$  calcd for  $C_{33}H_{43}N_4O_7S_2$ , 671.2568; found, 671.2574.

**(1*R*,3*aS*,7*aR*)-Octahydro-1,6-epoxyisobenzofuran-5-yl((2*S*,3*R*)-3-Hydroxy-4-((*N*-isobutyl-2-isopropylamino)benzo- $[d]$ oxazole)-6-sulfonamido)-1-phenylbutan-2-yl)carbamate (4c).**

Activated alcohol **16** (10 mg, 0.031 mmol) was treated with isostere amine **22** (16 mg, 0.034 mmol) by following the procedure outlined for inhibitor **4a** to give inhibitor **4c** (17.5 mg, 86%) as an amorphous solid.  $R_f = 0.4$  (5% MeOH/ $CH_2Cl_2$ ).  $^1H$  NMR (800 MHz,  $CDCl_3$ ):  $\delta$  7.71 (d,  $J = 1.8$  Hz, 1H), 7.64 (dd,  $J = 8.2, 1.8$  Hz, 1H), 7.41 (d,  $J = 8.3$  Hz, 1H), 7.31–7.25 (m, 5H), 7.23–7.19 (m, 1H), 5.61 (d,  $J = 3.6$  Hz, 1H), 5.44 (br s, 1H), 5.09 (d,  $J = 9.3$  Hz, 1H), 4.72 (t,  $J = 6.3$  Hz, 1H), 4.33 (t,  $J = 5.4$  Hz, 1H), 4.16–4.09 (m, 2H), 3.91–3.74 (m, 4H), 3.20 (dd,  $J = 15.1, 8.8$  Hz, 1H), 3.15–3.07 (m, 2H), 3.01 (dd,  $J = 13.4, 8.4$  Hz, 1H), 2.85–2.79 (m, 2H), 2.74 (dd,  $J = 8.8, 4.3$  Hz, 1H), 2.52 (m, 1H), 1.97 (dt,  $J = 12.6, 4.7$  Hz, 1H), 1.90–1.85 (m, 2H), 1.81 (br s, 1H), 1.72 (d,  $J = 12.6$  Hz, 1H), 1.38 (d,  $J = 6.5$  Hz, 6H), 1.31–1.27 (m, 1H), 0.94 (d,  $J = 6.6$  Hz, 3H), 0.89 (d,  $J = 6.6$  Hz, 3H);  $^{13}C$  NMR (200 MHz,  $CDCl_3$ ):  $\delta$  163.3, 155.9, 147.9, 147.7, 137.8, 130.0, 129.5, 128.4, 126.4, 124.2, 116.0, 108.9, 108.5, 76.4, 75.4, 72.4, 58.8, 55.2, 53.7, 45.7, 42.6, 36.1, 34.2, 29.4, 29.1, 27.3, 23.0, 20.2, 19.9. LRMS-ESI ( $m/z$ ): 657.2  $[M + H]^+$ ; HRMS-ESI ( $m/z$ ):  $[M + H]^+$  calcd for  $C_{33}H_{45}N_4O_8S$ , 657.2953; found, 657.2947.

**(1*R*,3*aS*,7*aR*)-Octahydro-1,6-epoxyisobenzofuran-5-yl((2*S*,3*R*)-4-((2-(Cyclopropylamino)-*N*-isobutylbenzo- $[d]$ -thiazole)-6-sulfonamido)-1-(3,5-difluorophenyl)-3-hydroxybutan-2-yl)carbamate (4d).**

Activated alcohol **16** (7 mg, 0.021 mmol) was treated with isostere amine **19** (13 mg, 0.023 mmol) by following the procedure outlined for inhibitor **4a** to give inhibitor **4d** (10 mg, 65%) as an amorphous solid.  $R_f = 0.1$  (70% EtOAc/hexanes).  $^1H$  NMR (500 MHz,  $CDCl_3$ ):  $\delta$  8.11 (s, 1H), 7.71 (d,  $J = 10.0$  Hz, 1H), 7.57 (d,  $J = 8.5$  Hz, 1H), 6.90 (br s, 1H), 6.80 (d,  $J = 7.6$  Hz, 2H), 6.64 (dd,  $J = 10.1, 7.7$  Hz, 1H), 5.60 (d,  $J = 3.6$  Hz, 1H), 5.13 (d,  $J = 8.9$  Hz, 1H), 4.73 (m, 1H), 4.32 (t,  $J = 5.2$  Hz, 1H), 4.13 (t,  $J = 8.1$  Hz, 1H), 3.96–3.76 (m, 3H), 3.22–3.07 (m, 3H), 3.02 (dd,  $J = 13.4, 8.4$  Hz, 1H), 2.85 (dd,  $J = 13.4, 6.8$  Hz, 1H), 2.81–2.70 (m, 3H), 2.53 (m, 1H), 2.03–1.80 (m, 4H), 1.71 (d,  $J = 12.6$  Hz, 1H), 1.34 (d,  $J = 16.0$  Hz, 1H), 0.97–0.91 (m, 5H), 0.89 (d,  $J = 6.5$  Hz, 3H), 0.82–0.76 (m, 2H);  $^{13}C$  NMR (200 MHz,  $CDCl_3$ ):  $\delta$  172.8, 163.5 (d,  $J = 12.7$  Hz), 162.3 (d,  $J = 12.8$  Hz), 155.8, 155.6, 142.2 (m), 131.3, 130.6, 125.4, 121.0, 118.7, 112.4 (d,  $J = 20.6$  Hz), 108.9, 101.9 (t,  $J = 25.1$  Hz), 76.4, 75.3, 72.6, 72.4, 59.0, 55.0, 53.7, 42.5, 35.9, 34.2, 29.7, 29.4, 29.1, 27.4, 26.7, 20.2, 19.9, 8.0. LRMS-ESI ( $m/z$ ): 707.2  $[M + H]^+$ ; HRMS-ESI ( $m/z$ ):  $[M + H]^+$  calcd for  $C_{33}H_{41}F_2N_4O_7S_2$ , 707.2379; found, 707.2385.

**(1*R*,3*aS*,7*aR*)-Octahydro-1,6-epoxyisobenzofuran-5-yl((2*S*,3*R*)-4-((2-(Cyclopropylamino)-*N*-isobutylbenzo- $[d]$ -thiazole)-6-sulfonamido)-1-(3-fluorophenyl)-3-hydroxybutan-2-yl)carbamate (4e).**

Activated alcohol **16** (12 mg, 0.037 mmol) was treated with isostere amine **20** (21 mg, 0.041 mmol) by following the procedure outlined for inhibitor **4a** to give inhibitor **4e** (18 mg, 70%) as an amorphous solid.  $R_f = 0.2$  (80% EtOAc/hexanes).  $^1H$  NMR (500 MHz,  $CDCl_3$ ):

$\delta$  8.13 (d,  $J = 1.9$  Hz, 1H), 7.74 (dd,  $J = 8.4, 2.0$  Hz, 1H), 7.59 (d,  $J = 8.9$  Hz, 1H), 7.26 (dd,  $J = 8.1, 6.2$  Hz, 1H), 7.18 (br s, 1H), 7.07 (d,  $J = 7.7$  Hz, 1H), 7.00 (m, 1H), 6.92 (t,  $J = 8.6$  Hz, 1H), 5.63 (d,  $J = 3.7$  Hz, 1H), 5.10 (d,  $J = 9.2$  Hz, 1H), 4.75 (m, 1H), 4.35 (t,  $J = 5.6$  Hz, 1H), 4.14 (t,  $J = 8.3$  Hz, 1H), 3.94–3.77 (m, 4H), 3.23 (dd,  $J = 15.2, 8.4$  Hz, 1H), 3.20–3.07 (m, 2H), 3.05 (dd,  $J = 13.4, 8.3$  Hz, 1H), 2.91–2.71 (m, 4H), 2.54 (m, 1H), 2.07–1.85 (m, 4H), 1.73 (d,  $J = 12.8$  Hz, 1H), 1.34 (d,  $J = 10.0$  Hz, 1H), 1.00–0.88 (m, 8H), 0.84–0.80 (m, 2H);  $^{13}\text{C}$  NMR (200 MHz,  $\text{CDCl}_3$ ):  $\delta$  172.9, 163.4 (d,  $J = 9.4$  Hz), 162.2 (d,  $J = 10.1$  Hz), 155.9, 155.5, 140.6 (d,  $J = 5.9$  Hz), 131.2, 130.7, 129.8 (d,  $J = 8.3$  Hz), 125.4 (d,  $J = 33.8$  Hz), 121.0, 118.7, 116.4 (d,  $J = 21.0$  Hz), 113.3 (d,  $J = 21.0$  Hz), 108.9, 76.4, 75.4, 72.5, 72.5, 58.9, 55.1, 53.7, 42.5, 35.9, 34.2, 31.9, 29.7, 29.5, 29.4, 29.4, 29.1, 27.3, 26.7, 20.2, 19.9, 8.0. LRMS-ESI ( $m/z$ ): 689.2 [ $\text{M} + \text{H}$ ] $^+$ ; HRMS-ESI ( $m/z$ ): [ $\text{M} + \text{H}$ ] $^+$  calcd for  $\text{C}_{33}\text{H}_{42}\text{FN}_4\text{O}_7\text{S}_2$ , 689.2474; found, 689.2466.

**(1*R*,3*aS*,7*aR*)-Octahydro-1,6-epoxyisobenzofuran-5-yl((2*S*,3*R*)-4-((2-(Cyclopropylamino)-*N*-isobutylbenzo[*d*]-thiazole)-6-sulfonamido)-1-(4-fluorophenyl)-3-hydroxybutan-2-yl)carbamate (4f).**

Activated alcohol **16** (12 mg, 0.037 mmol) was treated with isostere amine **21** (21 mg, 0.041 mmol) by following the procedure outlined for inhibitor **4a** to give inhibitor **4f** (17.5 mg, 68%) as an amorphous solid.  $R_f = 0.2$  (80% EtOAc/hexanes).  $^1\text{H}$  NMR (500 MHz,  $\text{CDCl}_3$ ):  $\delta$  8.10 (d,  $J = 1.9$  Hz, 1H), 7.70 (dd,  $J = 8.5, 1.9$  Hz, 1H), 7.57 (d,  $J = 8.5$  Hz, 1H), 7.25–7.18 (m, 2H), 7.00–6.94 (m, 2H), 6.89 (br s, 1H), 5.60 (d,  $J = 3.6$  Hz, 1H), 5.02 (d,  $J = 9.0$  Hz, 1H), 4.70 (t,  $J = 6.1$  Hz, 1H), 4.33 (t,  $J = 5.4$  Hz, 1H), 4.11 (t,  $J = 8.2$  Hz, 1H), 3.92–3.71 (m, 4H), 3.18 (dd,  $J = 15.1, 8.2$  Hz, 1H), 3.14–3.06 (m, 2H), 3.01 (dd,  $J = 13.4, 8.5$  Hz, 1H), 2.83 (dd,  $J = 13.4, 6.7$  Hz, 1H), 2.79–2.70 (m, 3H), 2.52 (m, 1H), 1.96 (dt,  $J = 12.5, 5.2$  Hz, 1H), 1.92–1.81 (m, 2H), 1.70 (d,  $J = 12.6$  Hz, 1H), 1.29 (d,  $J = 10.0$  Hz, 1H), 0.98–0.90 (m, 5H), 0.88 (d,  $J = 6.6$  Hz, 3H), 0.82–0.77 (m, 2H);  $^{13}\text{C}$  NMR (200 MHz,  $\text{CDCl}_3$ ):  $\delta$  172.9, 162.2, 161.0, 156.0, 133.6, 131.0 (d,  $J = 8.0$  Hz), 130.7, 125.4, 121.0, 118.7, 115.2 (d,  $J = 21.0$  Hz), 108.9, 76.4, 75.4, 72.6, 72.5, 58.9, 55.3, 53.7, 42.6, 35.2, 34.2, 29.7, 29.4, 29.1, 27.3, 26.7, 20.2, 19.9, 8.0. LRMS-ESI ( $m/z$ ): 689.2 [ $\text{M} + \text{H}$ ] $^+$ ; HRMS-ESI ( $m/z$ ): [ $\text{M} + \text{H}$ ] $^+$  calcd for  $\text{C}_{33}\text{H}_{42}\text{FN}_4\text{O}_7\text{S}_2$ , 689.2474; found, 689.2481.

**(1*S*,3*aR*,5*S*,7*aS*)-Octahydro-1,6-epoxyisobenzofuran-5-yl((2*S*,3*R*)-3-Hydroxy-4-((*N*-isobutyl-4-methoxyphenyl)-sulfonamido)-1-phenylbutan-2-yl)carbamate (5a).**

Activated alcohol *ent*-**16** (15 mg, 0.046 mmol) was treated with isostere amine **17** (21 mg, 0.051 mmol) by following the procedure outlined for inhibitor **4a** to give inhibitor **5a** (22 mg, 80%) as an amorphous solid.  $R_f = 0.3$  (70% EtOAc/hexanes).  $^1\text{H}$  NMR (800 MHz,  $\text{CDCl}_3$ ):  $\delta$  7.72 (d,  $J = 8.4$  Hz, 2H), 7.33–7.25 (m, 4H), 7.22 (t,  $J = 7.2$  Hz, 1H), 6.98 (d,  $J = 8.4$  Hz, 2H), 5.65 (s, 1H), 5.17 (d,  $J = 8.8$  Hz, 1H), 4.80–4.68 (m, 1H), 4.33 (t,  $J = 5.4$  Hz, 1H), 4.13 (m, 1H), 3.88 (s, 3H), 3.91–3.75 (m, 4H), 3.13–2.91 (m, 4H), 2.87–2.71 (m, 2H), 2.56 (m, 1H), 2.06–1.68 (m, 5H), 1.52 (d,  $J = 15.8$  Hz, 1H), 1.31 (m, 1H), 0.91 (d,  $J = 6.6$  Hz, 3H), 0.87 (d,  $J = 6.7$  Hz, 3H);  $^{13}\text{C}$  NMR (200 MHz,  $\text{CDCl}_3$ ):  $\delta$  162.9, 156.2, 137.8, 130.1, 129.6, 129.5, 128.5, 126.4, 114.3, 108.9, 76.6, 75.7, 72.6, 72.1, 58.6, 55.6, 55.4, 53.5, 42.7, 35.2, 34.3, 29.7, 29.5, 29.5, 27.2, 20.1, 19.9. LRMS-ESI ( $m/z$ ): 589.2 [ $\text{M} + \text{H}$ ] $^+$ ; HRMS-ESI ( $m/z$ ): [ $\text{M} + \text{H}$ ] $^+$  calcd for  $\text{C}_{30}\text{H}_{40}\text{N}_2\text{O}_8\text{SNa}$ , 611.2398; found, 611.2410.

**(1*S*,3*aR*,5*S*,7*aS*)-Octahydro-1,6-epoxyisobenzofuran-5-yl((2*S*,3*R*)-4-((2-(Cyclopropylamino)-*N*-isobutylbenzo[*d*]thiazole)-6-sulfonamido)-3-hydroxy-1-phenylbutan-2-yl)-carbamate (5b).**

Activated alcohol *ent*-**16** (15 mg, 0.046 mmol) was treated with isostere amine **18** (25 mg, 0.051 mmol) by following the procedure outlined for inhibitor **4a** to give inhibitor **5b** (22 mg, 70%) as an amorphous solid.  $R_f = 0.2$  (80% EtOAc/hexanes).  $^1\text{H NMR}$  (800 MHz,  $\text{CDCl}_3$ ):  $\delta$  8.08 (s, 1H), 7.69 (d,  $J = 8.5$  Hz, 1H), 7.57 (d,  $J = 8.5$  Hz, 1H), 7.32–7.26 (m, 5H), 7.24–7.16 (m, 2H), 5.65 (d,  $J = 3.6$  Hz, 1H), 5.19 (d,  $J = 8.8$  Hz, 1H), 4.78 (t,  $J = 6.1$  Hz, 1H), 4.34 (t,  $J = 5.4$  Hz, 1H), 4.13 (t,  $J = 8.3$  Hz, 1H), 3.98–3.81 (m, 4H), 3.15 (dd,  $J = 15.0, 8.7$  Hz, 1H), 3.10–2.95 (m, 3H), 2.85 (dd,  $J = 13.5, 6.9$  Hz, 1H), 2.80–2.70 (m, 2H), 2.55 (m, 1H), 2.05–1.67 (m, 5H), 1.52 (d,  $J = 15.8$  Hz, 1H), 0.97 (d,  $J = 6.5$  Hz, 2H), 0.92 (d,  $J = 6.6$  Hz, 3H), 0.88 (d,  $J = 6.6$  Hz, 3H), 0.81 (m, 2H);  $^{13}\text{C NMR}$  (200 MHz,  $\text{CDCl}_3$ ):  $\delta$  172.98, 156.19, 155.60, 137.81, 131.20, 130.60, 129.62, 128.49, 126.49, 125.40, 120.93, 118.55, 108.88, 76.59, 75.67, 72.67, 72.20, 58.71, 55.48, 53.63, 42.72, 35.24, 34.32, 29.71, 29.50, 27.31, 26.68, 20.18, 19.91, 7.97. LRMS-ESI ( $m/z$ ): 671.2 [M + H] $^+$ ; HRMS-ESI ( $m/z$ ): [M + H] $^+$  calcd for  $\text{C}_{33}\text{H}_{43}\text{N}_4\text{O}_7\text{S}_2$ , 671.2568; found, 671.2563.

**(1*S*,3*aR*,5*S*,7*aS*)-Octahydro-1,6-epoxyisobenzofuran-5-yl((2*S*,3*R*)-3-Hydroxy-4-((*N*-isobutyl-2-(isopropylamino)benzo[*d*]oxazole)-6-sulfonamido)-1-phenylbutan-2-yl)carbamate (5c).**

Activated alcohol *ent*-**16** (8 mg, 0.024 mmol) was treated with isostere amine **22** (13 mg, 0.027 mmol) by following the procedure outlined for inhibitor **4a** to give inhibitor **5c** (14 mg, 86%) as an amorphous solid.  $R_f = 0.4$  (5% MeOH/ $\text{CH}_2\text{Cl}_2$ ).  $^1\text{H NMR}$  (800 MHz,  $\text{CDCl}_3$ ):  $\delta$  7.66 (s, 1H), 7.60 (d,  $J = 8.2$  Hz, 1H), 7.39 (d,  $J = 8.2$  Hz, 1H), 7.30–7.23 (m, 5H), 7.20 (t,  $J = 7.1$  Hz, 1H), 5.63 (d,  $J = 3.5$  Hz, 1H), 5.23 (br s, 1H), 5.07 (d,  $J = 8.9$  Hz, 1H), 4.76 (m, 1H), 4.32 (m, 1H), 4.15–4.05 (m, 2H), 3.87–3.72 (m, 4H), 3.13–2.92 (m, 4H), 2.85–2.67 (m, 2H), 2.53 (m, 1H), 2.03–1.95 (m, 2H), 1.92–1.77 (m, 2H), 1.73 (d,  $J = 12.5$  Hz, 1H), 1.50 (d,  $J = 15.8$  Hz, 1H), 1.36 (d,  $J = 6.5$  Hz, 6H), 0.90 (d,  $J = 6.6$  Hz, 3H), 0.86 (d,  $J = 6.6$  Hz, 3H);  $^{13}\text{C NMR}$  (200 MHz,  $\text{CDCl}_3$ ):  $\delta$  163.3, 156.2, 147.9, 137.7, 130.1, 129.6, 128.5, 126.5, 124.2, 116.0, 108.9, 108.4, 76.6, 75.7, 72.7, 72.1, 58.7, 56.0, 55.4, 53.7, 45.8, 42.7, 35.3, 34.3, 29.7, 29.5, 27.3, 23.0, 20.2, 19.9. LRMS-ESI ( $m/z$ ): 657.2 [M + H] $^+$ ; HRMS-ESI ( $m/z$ ): [M + H] $^+$  calcd for  $\text{C}_{33}\text{H}_{45}\text{N}_4\text{O}_8\text{S}$ , 657.2953; found, 657.2948.

**(1*S*,3*aR*,5*S*,7*aS*)-Octahydro-1,6-epoxyisobenzofuran-5-yl((2*S*,3*R*)-4-((2-(Cyclopropylamino)-*N*-isobutylbenzo[*d*]thiazole)-6-sulfonamido)-1-(3,5-difluorophenyl)-3-hydroxy-butan-2-yl)carbamate (5d).**

Activated alcohol *ent*-**16** (12 mg, 0.037 mmol) was treated with isostere amine **19** (21 mg, 0.041 mmol) by following the procedure outlined for inhibitor **4a** to give inhibitor **5d** (15.5 mg, 59%) as an amorphous solid.  $R_f = 0.3$  (5% MeOH/ $\text{CH}_2\text{Cl}_2$ ).  $^1\text{H NMR}$  (800 MHz,  $\text{CDCl}_3$ ):  $\delta$  8.11 (s, 1H), 7.72 (d,  $J = 8.6$  Hz, 1H), 7.59 (d,  $J = 8.5$  Hz, 1H), 6.98 (br s, 1H), 6.87–6.80 (m, 2H), 6.67 (m, 1H), 5.65 (d,  $J = 3.6$  Hz, 1H), 5.25 (d,  $J = 8.8$  Hz, 1H), 4.83–4.73 (m, 1H), 4.36 (t,  $J = 5.4$  Hz, 1H), 4.16–4.05 (m, 2H), 3.95–3.73 (m, 3H), 3.18–2.93 (m, 4H), 2.89 (dd,  $J = 13.3, 6.9$  Hz, 1H), 2.84–2.72 (m, 3H), 2.56 (q,  $J = 8.2$  Hz, 1H), 2.05–1.95 (m, 2H), 1.94–1.83 (m, 2H), 1.76 (d,  $J = 12.6$  Hz, 1H), 1.72 (m, 1H), 1.52 (d,  $J = 15.9$  Hz, 1H), 0.97 (d,  $J = 6.6$  Hz, 2H), 0.94 (d,  $J = 6.5$  Hz, 3H), 0.90 (d,  $J = 6.9$  Hz, 3H), 0.83–0.79

(m, 2H).  $^{13}\text{C}$  NMR (200 MHz,  $\text{CDCl}_3$ ):  $\delta$  173.0, 163.6 (d,  $J$  = 11.8 Hz), 162.3 (d,  $J$  = 12.1 Hz), 156.2, 155.6, 142.2 (m), 131.3, 130.4, 125.4, 120.9, 118.7, 112.4 (d,  $J$  = 20.2 Hz), 108.9, 102.0 (t,  $J$  = 24.2 Hz), 76.5, 75.5, 72.7, 72.3, 59.0, 55.3, 53.7, 42.6, 34.8, 34.3, 29.7, 29.5, 27.4, 26.7, 20.2, 19.9, 8.0. LRMS-ESI ( $m/z$ ): 707.2  $[\text{M} + \text{H}]^+$ ; HRMS-ESI ( $m/z$ ):  $[\text{M} + \text{H}]^+$  calcd for  $\text{C}_{33}\text{H}_{41}\text{F}_2\text{N}_4\text{O}_7\text{S}_2$ , 707.2379; found, 707.2384.

**(1S,3aR,5S,7aS)-Octahydro-1,6-epoxyisobenzofuran-5-yl((2S,3R)-4-((2-(Cyclopropylamino)-N-isobutylbenzo[d]thiazole)-6-sulfonamido)-1-(3-fluorophenyl)-3-hydroxybutan-2-yl)carbamate (5e).**

Activated alcohol *ent*-**16** (4 mg, 0.012 mmol) was treated with isostere amine **20** (7 mg, 0.013 mmol) by following the procedure outlined for inhibitor **4a** to give inhibitor **5e** (7.5 mg, 87%) as an amorphous solid.  $R_f$  = 0.2 (80% EtOAc/hexanes).  $^1\text{H}$  NMR (800 MHz,  $\text{CDCl}_3$ ):  $\delta$  8.14–8.07 (m, 1H), 7.73–7.65 (m, 1H), 7.56 (dd,  $J$  = 8.3, 2.8 Hz, 1H), 7.23 (m, 1H), 7.08–7.00 (m, 2H), 6.98 (d,  $J$  = 10.2 Hz, 1H), 6.89 (td,  $J$  = 8.8, 3.3 Hz, 1H), 5.63 (d,  $J$  = 3.6 Hz, 1H), 5.21 (d,  $J$  = 8.8 Hz, 1H), 4.77 (t,  $J$  = 6.3 Hz, 1H), 4.32 (t,  $J$  = 5.2 Hz, 1H), 4.11 (td,  $J$  = 8.9, 8.5, 3.2 Hz, 1H), 4.02–3.73 (m, 4H), 3.15–2.92 (m, 4H), 2.85 (dd,  $J$  = 13.3, 6.7 Hz, 1H), 2.79–2.70 (m, 2H), 2.57–2.48 (m, 1H), 2.01–1.93 (m, 2H), 1.89–1.81 (m, 2H), 1.73 (d,  $J$  = 12.5 Hz, 1H), 1.50 (d,  $J$  = 15.8 Hz, 1H), 0.95–0.84 (m, 8H), 0.81–0.77 (m, 2H);  $^{13}\text{C}$  NMR (200 MHz,  $\text{CDCl}_3$ ):  $\delta$  173.0, 163.4, 162.2, 156.2, 155.6, 140.6, 131.2, 130.6, 130.5, 129.9–125.7 (m), 125.5–125.2 (m), 120.9 (d,  $J$  = 8.5 Hz), 118.6, 116.5 (d,  $J$  = 22.9 Hz), 113.4 (t,  $J$  = 19.0 Hz), 108.9, 76.5 (d,  $J$  = 36.1 Hz), 75.5 (d,  $J$  = 35.0 Hz), 72.7, 72.3, 58.8, 55.4, 55.2, 53.6, 42.7, 42.5, 34.8, 34.3, 34.2, 29.7, 29.5, 29.4, 29.1, 27.3, 26.7, 20.2, 19.9, 8.0. LRMS-ESI ( $m/z$ ): 689.2  $[\text{M} + \text{H}]^+$ ; HRMS-ESI ( $m/z$ ):  $[\text{M} + \text{H}]^+$  calcd for  $\text{C}_{33}\text{H}_{42}\text{FN}_4\text{O}_7\text{S}_2$ , 689.2474; found, 689.2481.

**(1S,3aR,5S,7aS)-Octahydro-1,6-epoxyisobenzofuran-5-yl((2S,3R)-4-((2-(Cyclopropylamino)-N-isobutylbenzo[d]thiazole)-6-sulfonamido)-1-(4-fluorophenyl)-3-hydroxybutan-2-yl)carbamate (5f).**

Activated alcohol *ent*-**16** (4 mg, 0.012 mmol) was treated with isostere amine **21** (7 mg, 0.013 mmol) by following the procedure outlined for inhibitor **4a** to give inhibitor **5f** (6.6 mg, 77%) as an amorphous solid.  $R_f$  = 0.2 (80% EtOAc/hexanes).  $^1\text{H}$  NMR (800 MHz,  $\text{CDCl}_3$ ):  $\delta$  8.07 (s, 1H), 7.67 (d,  $J$  = 8.6 Hz, 1H), 7.56 (d,  $J$  = 8.5 Hz, 1H), 7.25–7.20 (m, 2H), 6.98–6.95 (m, 2H), 6.83 (br s, 1H), 5.63 (d,  $J$  = 3.5 Hz, 1H), 5.10 (d,  $J$  = 9.1 Hz, 1H), 4.74 (m, 1H), 4.32 (t,  $J$  = 5.5 Hz, 1H), 4.11 (t,  $J$  = 7.9 Hz, 1H), 3.90–3.72 (m, 4H), 3.12 (dd,  $J$  = 15.0, 8.5 Hz, 1H), 3.07–3.03 (m, 1H), 3.01–2.96 (m, 2H), 2.91 (dd,  $J$  = 14.2, 8.2 Hz, 1H), 2.83 (dd,  $J$  = 13.5, 6.8 Hz, 1H), 2.77–2.69 (m, 2H), 2.53 (m, 1H), 2.03–1.95 (m, 2H), 1.89–1.80 (m, 2H), 1.73 (d,  $J$  = 12.5 Hz, 1H), 1.48 (d,  $J$  = 15.8 Hz, 1H), 0.96–0.93 (m, 2H), 0.91 (d,  $J$  = 6.6 Hz, 3H), 0.86 (d,  $J$  = 6.7 Hz, 3H), 0.81–0.78 (m, 2H);  $^{13}\text{C}$  NMR (200 MHz,  $\text{CDCl}_3$ ):  $\delta$  172.9, 162.3, 161.1, 156.1, 155.5, 133.4, 131.2, 131.1–131.0 (m), 130.6, 125.4, 120.9, 118.7, 115.2 (d,  $J$  = 20.9 Hz), 108.9, 76.6, 75.5, 72.7, 72.1, 58.8, 55.4, 53.7, 42.7, 34.5, 34.3, 29.7, 29.5, 29.4, 27.3, 26.7, 20.2, 19.9, 8.0. LRMS-ESI ( $m/z$ ): 689.2  $[\text{M} + \text{H}]^+$ ; HRMS-ESI ( $m/z$ ):  $[\text{M} + \text{H}]^+$  calcd for  $\text{C}_{33}\text{H}_{42}\text{FN}_4\text{O}_7\text{S}_2$ , 689.2474; found, 689.2478.

**(1*R*,3*aS*,5*S*,7*aR*)-Octahydro-1,6-epoxyisobenzofuran-5-ol (6).**

To a stirred solution of triol **13** (340 mg, 1.54 mmol) in dichloromethane (16 mL) was added 10-camphorsulfonic acid (36 mg, 0.15 mmol) at 0 °C for 1 h. The crude residue was purified by silica gel column chromatography (40% EtOAc/hexanes) to afford alcohol **6** (198 mg, 82%) as a white amorphous solid.  $R_f = 0.3$  (70% EtOAc/hexanes).  $[\alpha]_D^{20} + 45.5$  ( $c$  0.77, CHCl<sub>3</sub>). <sup>1</sup>H NMR (400 MHz, CDCl<sub>3</sub>):  $\delta$  5.64 (d,  $J = 4.2$  Hz, 1H), 4.30 (t,  $J = 5.7$  Hz, 1H), 4.03–3.87 (m, 3H), 3.21 (d,  $J = 10.3$  Hz, 1H), 2.82 (dt,  $J = 8.8, 4.4$  Hz, 1H), 2.56–2.48 (m, 1H), 1.93 (dt,  $J = 12.4, 5.0$  Hz, 1H), 1.83–1.73 (m, 2H), 1.56 (dt,  $J = 15.4, 1.1$  Hz, 1H); <sup>13</sup>C NMR (100 MHz, CDCl<sub>3</sub>):  $\delta$  108.6, 76.8, 76.6, 67.5, 42.1, 34.7, 31.8, 29.6. LRMS-ESI ( $m/z$ ): 157 [M + H]<sup>+</sup>.

**(1*S*,3*aR*,7*aS*)-Octahydro-1,6-epoxyisobenzofuran-5-ol (*ent*-6).**

The title compound *ent*-**6** (62 mg, 79%) was obtained from *ent*-**13** (110 mg, 0.5 mmol) by following the procedure outlined for compound **6**.  $R_f = 0.3$  (70% EtOAc/hexanes);  $[\alpha]_D^{20} = -47.3$  ( $c$  0.76, CHCl<sub>3</sub>). <sup>1</sup>H and <sup>13</sup>C NMR data is identical with **6**.

***cis*-Cyclohex-4-ene-1,2-dimethanol (9).**

To a slurry of lithium aluminum hydride in THF was added *cis*-4-cyclohexene-1,2-dicarboxylic anhydride **10** (7 g, 46.00 mmol) in THF (300 mL) at 0 °C over 20 min. The reaction mixture was stirred at 0 °C for 3 h and quenched by dropwise addition of methanol over a period of 30 min at 0 °C. The reaction mixture was allowed to warm to room temperature, and aq solution of sodium sulfate was added and stirred at 23 °C overnight. The resulting slurry was filtered, and the solid was rinsed with ethyl acetate. The layers were separated, and the aqueous layer was extracted with ethyl acetate. The combined organic layers were dried over Na<sub>2</sub>SO<sub>4</sub>, filtered, and the solvent was removed under reduced pressure to give *cis*-diol **9** (g, 85%) as liquid. <sup>1</sup>H NMR (400 MHz, CDCl<sub>3</sub>):  $\delta$  5.62–5.59 (m, 2H), 3.71 (dd,  $J = 11.0, 6.5$  Hz, 2H), 3.58 (dd,  $J = 11.1, 3.3$  Hz, 2H), 3.27 (br s, 2H), 2.18–1.96 (m, 6H); <sup>13</sup>C NMR (101 MHz, CDCl<sub>3</sub>):  $\delta$  125.4, 64.0, 37.7, 26.8. LRMS-ESI ( $m/z$ ): 143.0 [M + H]<sup>+</sup>.

**((1*S*,6*R*)-6-(Hydroxymethyl)cyclohex-3-en-1-yl)methyl Acetate (11).**

A mixture of diol **9** (0.5 g, 3.52 mmol) and PPL (porcine pancreatic lipase Sigma type 2, 2.27 g) in ethyl acetate (50 mL) was stirred at 23 °C for 12 h. After completion of diol by TLC, the reaction mixture was filtered and the solvent was removed in *vacuo* to give a crude residue which was purified by column chromatography over silica gel (30% EtOAc/hexanes) to afford the mono acetate **11** (0.53 g, 82%) along with di acetate (40 mg, 5%) as the minor product.  $R_f = 0.5$  (50% EtOAc/hexanes).  $[\alpha]_D^{20} + 17.5$  ( $c$  2.2, CHCl<sub>3</sub>), {literature data:<sup>2</sup>  $[\alpha]_D^{20} + 19.0$  ( $c$  5.85, CHCl<sub>3</sub>)}; <sup>1</sup>H NMR (400 MHz, CDCl<sub>3</sub>):  $\delta$  5.67–5.57 (m, 2H), 4.17 (dd,  $J = 11.0, 6.0$  Hz, 1H), 3.94 (dd,  $J = 11.0, 8.0$  Hz, 1H), 3.68–3.53 (m, 2H), 2.27–2.20 (m, 1H), 2.17–2.05 (m, 3H), 2.04 (s, 3H), 2.03–1.82 (m, 3H). <sup>13</sup>C NMR (101 MHz, CDCl<sub>3</sub>):  $\delta$  171.3, 125.5, 125.0, 64.9, 63.5, 37.1, 33.1, 26.9, 25.9, 20.9. LRMS-ESI ( $m/z$ ): 185.1 [M + H]<sup>+</sup>. Spectral data was identical with the reported data.<sup>1</sup>



**((1R,6S)-6-(Hydroxymethyl)cyclohex-3-en-1-yl)methyl Acetate (*ent*-11).**

To a stirred solution of diacetate **15** (18.6 g, 82.30 mmol) in 0.1 M phosphate buffer (242 mL, pH 7) was added PPL (1.86 g, Sigma type II, crude) at 23 °C. NaHCO<sub>3</sub> solution (93 mL) (1 N) was added dropwise, and the heterogeneous mixture was stirred for 16 h. The mixture was then filtered through a pad of Celite. The filtrate was extracted with dichloromethane (×3). The combined organic layers were washed with brine, dried over Na<sub>2</sub>SO<sub>4</sub>, filtered, and the solvent was evaporated in *vacuo*. The residue was purified by chromatography over silica gel (30% EtOAc/hexanes) to obtain *ent*-**11** (12.75 g, 84%) as colorless oil. *R*<sub>f</sub> = 0.5 (50% EtOAc/hexanes). [ $\alpha$ ] = -17.5 (*c* = 1.43, CHCl<sub>3</sub>); LRMS-ESI (*m/z*): 185.1 [M + H]<sup>+</sup>. <sup>1</sup>H and <sup>13</sup>C NMR spectral data were identical with **11**.

**((1S,6R)-6-(Dimethoxymethyl)cyclohex-3-en-1-yl)methyl Acetate (**12**).**

Oxalyl chloride (1.34 mL, 15.21 mmol) in dry CH<sub>2</sub>Cl<sub>2</sub> (60 mL) was cooled to -78 °C under a nitrogen atmosphere. Dimethyl sulfoxide (2.2 mL, 30.43 mmol) was added dropwise. After 15 min, alcohol **11** (1.4 g, 7.60 mmol) in dry CH<sub>2</sub>Cl<sub>2</sub> (20 mL) was added to the reaction mixture *via* cannula and stirred for 30 min at -78 °C. Then, Et<sub>3</sub>N (5.3 mL, 38.04 mmol) was added and the mixture stirred for 15 min. Further reaction was carried out at 0 °C. The solvent was concentrated, extracted with EtOAc (2 × 100 mL), and washed with H<sub>2</sub>O and brine, and the organic layer was dried over Na<sub>2</sub>SO<sub>4</sub>, filtered, and concentrated under reduced pressure. The residue was purified by flash column chromatography (15% EtOAc/hexanes) to afford aldehyde **S1** (1.25 g, 90%) as colorless oil. *R*<sub>f</sub> = 0.5 (30% EtOAc/hexanes). [ $\alpha$ ]<sub>D</sub><sup>20</sup> = -47.9 (*c* 0.73, CHCl<sub>3</sub>); <sup>1</sup>H NMR (400 MHz, CDCl<sub>3</sub>):  $\delta$  9.71 (s, 1H), 5.73–5.61 (m, 2H), 4.12–4.03 (m, 2H), 2.65–2.55 (m, 2H), 2.33–2.24 (m, 3H), 2.07–1.96 (m, 4H); <sup>13</sup>C NMR (100 MHz, CDCl<sub>3</sub>):  $\delta$  203.2, 170.6, 125.3, 124.7, 64.4, 47.2, 32.7, 26.8, 22.6, 20.6. LRMS-ESI (*m/z*): 183.0 [M + H]<sup>+</sup>.

To a stirred solution of above aldehyde (1.25 g, 6.86 mmol) in methanol (20 mL) was added trimethyl orthoformate (7.5 mL, 68.60 mmol) followed by tetrabutylammonium tribromide (66 mg, 0.137 mmol) at 23 °C. The reaction mixture was stirred for 8 h at 23 °C. After this period, the reaction mixture was quenched by the addition of saturated aqueous NH<sub>4</sub>Cl solution. Methanol was removed under reduced pressure and the reaction mixture was diluted with ethyl acetate. The layers were separated, the aqueous layer was extracted with EtOAc, and combined organic extracts were dried over Na<sub>2</sub>SO<sub>4</sub> and concentrated under reduced pressure. The crude product was purified by silica gel column chromatography (10% EtOAc/hexanes) to afford **12** (1.32 g, 84%). *R*<sub>f</sub> = 0.5 (10% EtOAc/hexanes, 3 times). [ $\alpha$ ]<sub>D</sub><sup>20</sup> = +5.9 (*c* 1.2, CHCl<sub>3</sub>). <sup>1</sup>H NMR (400 MHz, CDCl<sub>3</sub>):  $\delta$  5.70–5.54 (m, 2H), 4.33 (dd, *J* = 8.3, 1.9 Hz, 1H), 4.12 (ddd, *J* = 10.8, 5.4, 1.8 Hz, 1H), 3.99 (ddd, *J* = 10.8, 9.0, 1.9 Hz, 1H), 3.36–3.30 (m, 6H), 2.29 (m, 1H), 2.21–1.99 (m, 7H), 1.88 (dddd, *J* = 16.1, 7.9, 4.3, 2.2 Hz, 1H); <sup>13</sup>C NMR (100 MHz, CDCl<sub>3</sub>):  $\delta$  171.1, 125.7, 124.7, 105.0, 64.3, 53.5, 52.5, 37.4, 31.9, 27.5, 24.5, 21.0. LRMS-ESI (*m/z*): 251.1 [M + Na]<sup>+</sup>.

**((1R,6S)-6-(Dimethoxymethyl)cyclohex-3-en-1-yl)methyl Acetate (*ent*-12).**

The title compound *ent*-**12** (9 g, 80% over two steps) was obtained from *ent*-**11** (9 g, 48.91 mmol) by following the procedure outlined for compound **12**. *R*<sub>f</sub> = 0.5 (10% EtOAc/

hexanes, 3 times).  $[\alpha]_{\text{D}}^{20} - 5.5$  ( $c$  1.0,  $\text{CHCl}_3$ ).  $^1\text{H}$  and  $^{13}\text{C}$  NMR spectral data were identical with **12**.

**(1R,2S,4R,5S)-4-(Dimethoxymethyl)-5-(hydroxymethyl)-cyclohexane-1,2-diol (13) and (1S,2R,4R,5S)-4-(Dimethoxy-methyl)-5-(hydroxymethyl)cyclohexane-1,2-diol (14).**

AD-mix- $\beta$  (3.0 g) was dissolved in 1:1 *tert*-butyl alcohol/water (22 mL), and the mixture was stirred for 10 min.  $\text{MeSO}_2\text{NH}_2$  (208 mg, 2.19 mmol) was then added, and stirring was continued for a further 10 min. After the mixture was cooled to 0 °C, **12** (500 mg, 2.19 mmol) in *t*-BuOH (2 mL) was added. The reaction was slowly warmed to ambient temperature and stirred for 24 h. At this time, solid  $\text{Na}_2\text{SO}_3$  was added, and the reaction was stirred for an additional 30 min. The reaction was then partitioned between EtOAc/water and the aqueous layer extracted with EtOAc. The combined organic layers were washed brine solution, dried over  $\text{Na}_2\text{SO}_4$ , filtered, and concentrated under reduced pressure to yield inseparable mixture of diols which were used for the next step with further purification.

The stirred solution of above diol was dissolved in methanol (6 mL), and 1 N NaOH (0.6 mL) at 0 °C was added. The reaction mixture was slowly warmed to ambient temperature and stirred for 3 h. After completion of the starting material, methanol was evaporated and extracted with dichloromethane ( $3 \times 30$  mL). The combined organic layers were dried over  $\text{Na}_2\text{SO}_4$ , filtered, and concentrated under reduced pressure. The crude residue was purified by column chromatography (5% MeOH/ $\text{CH}_2\text{Cl}_2$ ) over silica gel to afford triol **13** (207 mg, 43%) and **14** (227 mg, 47%) as an oily liquids.

**Compound 13.**

$R_f = 0.4$  (10% MeOH/ $\text{CH}_2\text{Cl}_2$ ).  $[\alpha]_{\text{D}}^{20} - 3.2$  ( $c$  0.58,  $\text{CHCl}_3$ ).  $^1\text{H}$  NMR (400 MHz, methanol- $d_4$ ):  $\delta$  4.46 (d,  $J = 8.3$  Hz, 1H), 3.82–3.72 (m, 2H), 3.60 (dd,  $J = 11.4, 4.3$  Hz, 1H), 3.55 (m, 1H), 3.36 (s, 3H), 3.35 (s, 3H), 2.00–1.82 (m, 3H), 1.81–1.69 (m, 2H), 1.62 (dt,  $J = 12.9, 4.3$  Hz, 1H);  $^{13}\text{C}$  NMR (100 MHz, methanol- $d_4$ ):  $\delta$  104.9, 70.7, 68.4, 62.9, 52.4, 52.1, 39.0, 34.6, 33.2, 27.4. LRMS-ESI ( $m/z$ ): 243.1  $[\text{M} + \text{Na}]^+$ .

**Compound 14.**

$R_f = 0.2$  (10% MeOH/ $\text{CH}_2\text{Cl}_2$ ).  $[\alpha]_{\text{D}}^{20} - 0.77$  ( $c$  3.49,  $\text{CHCl}_3$ ).  $^1\text{H}$  NMR (400 MHz, methanol- $d_4$ ):  $\delta$  4.30 (d,  $J = 7.8$  Hz, 1H), 3.89 (dt,  $J = 6.0, 3.0$  Hz, 1H), 3.77 (dt,  $J = 10.2, 3.7$  Hz, 1H), 3.63 (dd,  $J = 10.9, 6.0$  Hz, 1H), 3.50 (dd,  $J = 11.0, 8.8$  Hz, 1H), 3.33 (s, 3H), 3.31 (s, 3H), 2.26 (ddt,  $J = 12.0, 8.3, 4.2$  Hz, 1H), 2.15–2.07 (m, 1H), 1.87–1.79 (m, 1H), 1.78–1.65 (m, 2H), 1.63–1.51 (m, 1H).  $^{13}\text{C}$  NMR (100 MHz, MeOD):  $\delta$  105.2, 68.4, 67.3, 60.3, 52.7, 51.7, 35.8, 34.3, 28.8, 28.5. LRMS-ESI ( $m/z$ ): 243.1  $[\text{M} + \text{Na}]^+$ .

**(1S,2R,4S,5R)-4-(Dimethoxymethyl)-5-(hydroxymethyl)-cyclohexane-1,2-diol (ent-13) and (1R,2S,4S,5R)-4-(Dimethoxymethyl)-5-(hydroxymethyl)cyclohexane-1,2-diol (ent-14).**

Triol *ent*-**13** (405 mg, 42%) and *ent*-**14** (445 mg, 46%) were synthesized from *ent*-**12** (1 g, 4.38 mmol) by following the procedure outlined for compound **13** and **14**.

**cis-Cyclohex-4-ene-1,2-diylbis(methylene) Diacetate (15).**

To a stirred solution of diol **9** (11.5 g, 80.98 mmol) were added pyridine (26.1 mL, 323.94 mmol), acetic anhydride (15.3 mL, 161.97 mmol), and followed by DMAP (495 mg, 4.05 mmol) at 0 °C. The resulting mixture was stirred at 23 °C overnight. Upon completion, the reaction mixture was quenched with water and extracted with EtOAc (2 × 100 mL). The combined organic layers were dried over NaSO<sub>4</sub>, filtered, and concentrated under reduced pressure. The crude residue was purified by silica gel column chromatography (20% EtOAc/hexanes) to afford alcohol **15** (18.1 g, 98%).  $R_f = 0.8$  (50% EtOAc/hexanes). <sup>1</sup>H NMR (400 MHz, chloroform-*d*): δ 5.63–5.60 (m, 2H), 4.12–4.07 (m, 2H), 4.04–3.98 (m, 2H), 2.28–2.11 (m, 4H), 2.05 (s, 6H), 1.97–1.89 (m, 2H). <sup>13</sup>C NMR (101 MHz, CDCl<sub>3</sub>): δ 170.9, 125.0, 65.0, 33.6, 26.5, 20.9. LRMS-ESI (*m/z*): 227.1 [M + H]<sup>+</sup>.

**4-Nitrophenyl ((1*R*,3*aS*,7*aR*)-Octahydro-1,6-epoxyisobenzofuran-5-yl) Carbonate (16).**

To a stirred solution of **6** (22 mg, 0.14 mmol) in dichloromethane (1.0 mL) were added pyridine (30 μL, 0.32 mmol) and 4-nitrophenylchloroformate (63 mg, 0.31 mmol) at 0 °C under an argon atmosphere. The reaction mixture was warmed to 23 °C and stirred for 12 h. Upon completion, solvent was removed under reduced pressure. The crude product was purified by silica gel column chromatography (35% EtOAc in hexane) to afford **16** (39.5 mg, 87%) as an amorphous solid.  $R_f = 0.5$  (70% EtOAc/hexanes).  $[\alpha]_D^{20} + 77.4$  (*c* 0.7, CHCl<sub>3</sub>). <sup>1</sup>H NMR (500 MHz, CDCl<sub>3</sub>): δ 8.27–8.23 (m, 2H), 7.43–7.38 (m, 2H), 5.69 (d, *J* = 3.6 Hz, 1H), 4.91 (ddt, *J* = 7.4, 5.0, 1.0 Hz, 1H), 4.62 (t, *J* = 5.4 Hz, 1H), 4.18 (t, *J* = 8.3 Hz, 1H), 3.93 (dd, *J* = 8.8, 2.9 Hz, 1H), 2.82 (dt, *J* = 8.6, 3.9 Hz, 1H), 2.68–2.59 (m, 1H), 2.11–2.01 (m, 2H), 1.80 (d, *J* = 12.7 Hz, 1H), 1.71 (d, *J* = 14.7 Hz, 1H); <sup>13</sup>C NMR (125 MHz, CDCl<sub>3</sub>): δ 155.7, 151.7, 145.3, 125.2, 121.9, 109.1, 77.2, 76.2, 73.9, 42.3, 34.0, 29.2, 28.5. LRMS-ESI (*m/z*): 344 [M + Na]<sup>+</sup>.

**4-Nitrophenyl ((1*S*,3*aR*,7*aS*)-Octahydro-1,6-epoxyisobenzofuran-5-yl) Carbonate (*ent*-16).**

The title compound *ent*-**16** (100 mg, 88%) was obtained from *ent*-**6** (55 mg, 0.352 mmol) by following the procedure outlined for compound **16**.  $R_f = 0.5$  (70% EtOAc/hexanes).  $[\alpha]_D^{20} - 79.1$  (*c* 0.8, CHCl<sub>3</sub>). <sup>1</sup>H and <sup>13</sup>C NMR data are identical with **16**.

**Determination of X-ray structure of HIV-1 Protease–Inhibitor Complex.**

The HIV-1 protease was expressed and purified, as described previously.<sup>45</sup> The PR/5c complex was crystallized by the hanging drop vapor diffusion method with a well solution of 1.25 M NaCl and 0.1 M sodium acetate, pH 4.8, while PR/4a crystals were grown with a reservoir solution of 0.65 M NaCl and 0.1 M sodium acetate, pH 6.0. Diffraction data were collected on a single crystal cooled to 90 K at SER-CAT (22-BM beamline), Advanced Photon Source, Argonne National Lab (Chicago, USA) with an X-ray wavelength of 1.0 Å. The two data sets were processed by HKL-2000<sup>46</sup> to a Rmerge of 5.6 and 7.9%. The complex structures were solved by PHASER<sup>47</sup> in CCP4i Suite<sup>48–50</sup> using the previously determined isomorphous structure with PDB code 3NU3<sup>51</sup> as the start model. The PR/5c and PR/4a complexes were refined by SHELX-2014<sup>52,53</sup> up to 1.3 Å resolution and by REFMAC5<sup>54</sup> to 1.25 Å resolution. PRODRG-2<sup>55</sup> and Jligand<sup>56</sup> were used to construct

inhibitors and the restraints for refinement. COOT<sup>57,58</sup> was used for model building. Anisotropic atomic displacement parameters (B factors) were applied for all atoms including solvent molecules. The final refined solvent structure comprised one Na<sup>+</sup> ion, two Cl<sup>-</sup> ions, two acetate ion, and 189 water molecules for PR/5c and one Na<sup>+</sup> ion, two Cl<sup>-</sup> ions, one glycerol, one formic acid, and 222 water molecules for PR/4a. The crystallographic statistics are provided in the Supporting Information section. The coordinates and structure factors of PR/5c and PR/4a were deposited in the Protein Data Bank<sup>59</sup> with code 6VOE and 6VOD, respectively.

## Supplementary Material

Refer to Web version on PubMed Central for supplementary material.

## ACKNOWLEDGMENTS

This research was supported by the National Institutes of Health (Grant AI150466, A.K.G. and Grant AI150461, I.T.W.). X-ray data were collected at the Southeast Regional Collaborative Access Team (SER-CAT) beamline 22BM at the Advanced Photon Source, Argonne National Laboratory. Use of the Advanced Photon Source was supported by the US Department of Energy, Basic Energy Sciences, Office of Science, under contract no. W-31-109-Eng-38. This work was also supported by the Intramural Research Program of the Center for Cancer Research, National Cancer Institute, National Institutes of Health (H.M.), and in part by grants for the promotion of AIDS research from the Ministry of Health; grants from Welfare and Labor of Japan (H.M.); grants for the Research Program on HIV/AIDS from the Japan Agency for Medical Research and Development (AMED) under grant numbers JP15fk0410001 and JP16fk0410101 (H.M.); a grant from the National Center for Global Health and Medicine (NCGM) Research Institute (H.M.); and a Grant-in-Aid for Scientific Research (Priority Areas) from the Ministry of Education, Culture, Sports, Science, and Technology of Japan (Monbu Kagakusho) (H.M.). The authors would like to thank the Purdue University Center for Cancer Research, which supports the shared NMR and mass spectrometry facilities. The authors also thank M.A. for discussion.

## ABBREVIATIONS

<b>ART</b>	antiretroviral therapies
<b>ATV</b>	atazanavir
<b>Abt</b>	aminobenzothiazole
<b>bis-THF</b>	bis-tetrahydrofuran
<b>Chf-THF</b>	cyclohexane fused bis-tetrahydrofuran
<b>DIPEA</b>	<i>N,N</i> -diisopropyletamine
<b>DRV</b>	darunavir
<b>PI</b>	protease inhibitor

## REFERENCES

- (1). Lohse N; Hansen A-BE; Gerstoft J; Obel N Improved Survival in HIV-Infected Persons: Consequences and Perspectives. *J. Antimicrob. Chemother* 2007, 60, 461–463. [PubMed: 17609196]
- (2). Montaner JS; Lima VD; Barrios R; Yip B; Wood E; Kerr T; Shannon K; Harrigan PR; Hogg RS; Daly P; Kendall P Association of Highly Active Antiretroviral Therapy Coverage, Population

- Viral Load, and Yearly New HIV Diagnoses in British Columbia, Canada: A Population-Based Study. *Lancet* 2010, 376, 532–539. [PubMed: 20638713]
- (3). Kohl NE; Emini EA; Schleif WA; Davis LJ; Heimbach JC; Dixon RA; Scolnick EM; Sigal IS Active Human Immunodeficiency Virus Protease is Required for Viral Infectivity. *Proc. Natl. Acad. Sci. U.S.A* 1988, 85, 4686–4690. [PubMed: 3290901]
  - (4). Smith R; Brereton IM; Chai RY; Kent SBH Ionization States of the Catalytic Residues in HIV-1 Protease. *Nat. Struct. Mol. Biol* 1996, 3, 946–950.
  - (5). Blanco J-L; Varghese V; Rhee S-Y; Gatell JM; Shafer RW HIV-1 Integrase Inhibitor Resistance and Its Clinical Implications. *J. Infect. Dis* 2011, 203, 1204–1214. [PubMed: 21459813]
  - (6). Naggie S; Hicks C Protease Inhibitor-Based Antiretroviral Therapy in Treatment-Naive HIV-1-Infected Patients: The Evidence Behind the Options. *J. Antimicrob. Chemother* 2010, 65, 1094–1099. [PubMed: 20418273]
  - (7). Koh Y; Nakata H; Maeda K; Ogata H; Bilcer G; Devasamudram T; Kincaid JF; Boross P; Wang Y-F; Tie Y; Volarath P; Gaddis L; Harrison RW; Weber IT; Ghosh AK; Mitsuya H Novel bis-Tetrahydrofuranylurethane-Containing Non-peptidic Protease Inhibitor (PI) UIC-94017 (TMC114) with Potent Activity Against Multi-PI-Resistant Human Immunodeficiency Virus In Vitro. *Antimicrob. Agents Chemother* 2003, 47, 3123–3129. [PubMed: 14506019]
  - (8). De Meyer S; Azijn H; Surleraux D; Jochmans D; Tahri A; Pauwels R; Wigerinck P; de Béthune M-P TMC114, a Novel Human Immunodeficiency Virus Type 1 Protease Inhibitor Active Against Protease Inhibitor-Resistant Viruses, Including a Broad Range of Clinical Isolates. *Antimicrob. Agents Chemother* 2005, 49, 2314–2321. [PubMed: 15917527]
  - (9). de Béthune MP; Sekar V; Spinosa-Guzman S; Vanstockem M; De Meyer S; Wigerinck P; Lefebvre E Darunavir (Prezista, TMC114): From Bench to Clinic. *Improving Treatment Options for HIV-Infected Patients in Antiviral Drugs: From Basic Discovery through Clinical Trials*; John Wiley & Sons, Inc.: New Jersey, 2011; pp 31–45.
  - (10). Ghosh AK; Chapsal BD Design of the Anti-HIV-1 Protease Inhibitor Darunavir in *Introduction to Biological and Small Molecule Drug Research and Development: Theory and Case Studies*; Ganellin CR, Jefferis R, Roberts S, Eds.; Elsevier: London, 2013; pp 355–384.
  - (11). Lambert-Niclot S; Flandre P; Canestri A; Peytavin G; Blanc C; Agher R; Soulié C; Wirlden M; Katlama C; Calvez V; Marcelin A-G Factors Associated with the Selection of Mutations Conferring Resistance to Protease Inhibitors (PIs) in PI-experienced Patients Displaying Treatment Failure on Darunavir. *Antimicrob. Agents Chemother* 2008, 52, 491–496. [PubMed: 18039922]
  - (12). de Meyer S; Vangeneugden T; van Baelen B; de Paepe E; van Marck H; Picchio G; Lefebvre E; de Béthune M-P Resistance Profile of Darunavir: Combined 24-Week Results from the POWER Trials. *AIDS Res. Hum. Retroviruses* 2008, 24, 379–388. [PubMed: 18327986]
  - (13). Esté JA; Cihlar T Current Status and Challenges of Antiretroviral Research and Therapy. *Antiviral Res.* 2010, 85, 25–33. [PubMed: 20018390]
  - (14). Saylor D; Dickens AM; Sacktor N; Haughey N; Slusher B; Pletnikov M; Mankowski JL; Brown A; Volsky DJ; McArthur JC HIV-Associated Neurocognitive Disorder — Pathogenesis and Prospects for Treatment. *Nat. Rev. Neurol* 2016, 12, 234–248. [PubMed: 26965674]
  - (15). Ghosh AK; Ramu Sridhar P; Kumaragurubaran N; Koh Y; Weber IT; Mitsuya H Bis-Tetrahydrofuran: A Privileged Ligand for Darunavir and a New Generation of HIV Protease Inhibitors That Combat Drug Resistance. *ChemMedChem* 2006, 1, 939–950. [PubMed: 16927344]
  - (16). Ghosh AK; Anderson DD; Weber IT; Mitsuya H Enhancing Protein Backbone Binding—A Fruitful Concept for Combating Drug-Resistant HIV. *Angew. Chem., Int. Ed* 2012, 51, 1778–1802.
  - (17). Tie Y; Boross PI; Wang Y-F; Gaddis L; Hussain AK; Leshchenko S; Ghosh AK; Louis JM; Harrison RW; Weber IT High Resolution Crystal Structures of HIV-1 Protease with a Potent Non-peptide Inhibitor (UIC-94017) Active Against Multi-Drug-resistant Clinical Strains. *J. Mol. Biol* 2004, 338, 341–352. [PubMed: 15066436]

- (18). Kovalevsky AY; Liu F; Leshchenko S; Ghosh AK; Louis JM; Harrison RW; Weber IT Ultra-High Resolution Crystal Structure of HIV-1 Protease Mutant Reveals Two Binding Sites for Clinical Inhibitor TMC114. *J. Mol. Biol* 2006, 363, 161–173. [PubMed: 16962136]
- (19). Ghosh AK; Chapsal BD Aspartic Acid Proteases as Therapeutic Targets; Ghosh AK, Ed.; Wiley-VCH: Weinheim, Germany, 2010; pp 169–204.
- (20). Ghosh AK; Chapsal BD; Weber IT; Mitsuya H Design of HIV Protease Inhibitors Targeting Protein Backbone: An Effective Strategy for Combating Drug Resistance. *Acc. Chem. Res* 2008, 41, 78–86. [PubMed: 17722874]
- (21). Ghosh AK; Osswald HL; Prato G Recent Progress in the Development of HIV-1 Protease Inhibitors for the Treatment of HIV/AIDS. *J. Med. Chem* 2016, 59, 5172–5208. [PubMed: 26799988]
- (22). Ghosh AK; Nyalapatla, P. R, Kovala S; Rao KV; Brindisi M; Osswald HL; Amano M; Aoki M; Agniswamy J; Wang Y-F; Weber IT; Mitsuya H Design and Synthesis of Highly Potent HIV-1 Protease Inhibitors Containing Tricyclic Fused Ring Systems as Novel P2 Ligands: Structure–Activity Studies, Biological and X-ray Structural Analysis. *J. Med. Chem* 2018, 61, 4561–4577. [PubMed: 29763303]
- (23). Ghosh AK; Martyr CD; Osswald HL; Sheri VR; Kassekert LA; Chen S; Agniswamy J; Wang Y-F; Hayashi H; Aoki M; Weber IT; Mitsuya H Design of HIV-1 Protease Inhibitors with Amino-bis-Tetrahydrofuran Derivatives as P2-Ligands to Enhance Backbone-Binding Interactions: Synthesis, Biological Evaluation and Protein-Ligand X-ray Studies. *J. Med. Chem* 2015, 58, 6994–7006. [PubMed: 26306007]
- (24). Ghosh AK; Rao KV; Nyalapatla PR; Osswald HL; Martyr CD; Aoki M; Hayashi H; Agniswamy J; Wang Y-F; Bulut H; Das D; Weber IT; Mitsuya H Design and Development of Highly Potent HIV-1 Protease Inhibitors with a Crown-like Oxotricyclic Core as the P2-Ligand to Combat Multidrug-Resistant HIV Variants. *J. Med. Chem* 2017, 60, 4267–4278. [PubMed: 28418652]
- (25). Ghosh AK; Rao KV; Nyalapatla PR; Kovala S; Brindisi M; Osswald HL; Sekhara Reddy B; Agniswamy J; Wang Y-F; Aoki M; Hattori S.-i.; Weber IT; Mitsuya H Design of Highly Potent, Dual Acting and Central Nervous System Penetrating HIV-1 Protease Inhibitors with Excellent Potency against Multidrug-Resistant HIV-1 Variants. *ChemMedChem* 2018, 13, 803–815. [PubMed: 29437300]
- (26). Aoki M; Hayashi H; Rao KV; Das D; Higashi-Kuwata N; Bulut H; Aoki-Ogata H; Takamatsu Y; Yedidi RS; Davis DA; Hattori S.-i.; Nishida N; Hasegawa K; Takamune N; Nyalapatla PR; Osswald HL; Jono H; Saito H; Yarchoan R; Misumi S; Ghosh AK; Mitsuya H A Novel Central Nervous System-Penetrating Protease Inhibitor Overcomes Human Immunodeficiency Virus 1 Resistance with Unprecedented aM to pM potency. *eLife* 2017, 6, No. e28020. [PubMed: 29039736]
- (27). Hohlfeld K; Tomassi C; Wegner JK; Kesteleyn B; Linclau B Disubstituted Bis-THF Moieties as New P2 Ligands in Nonpeptidal HIV-1 Protease Inhibitors. *ACS Med. Chem. Lett* 2011, 2, 461–465. [PubMed: 24900331]
- (28). Hohlfeld K; Wegner JK; Kesteleyn B; Linclau B; Unge J Disubstituted Bis-THF Moieties as New P2 Ligands in Nonpeptidal HIV-1 Protease Inhibitors (II). *J. Med. Chem* 2015, 58, 4029–4038. [PubMed: 25897791]
- (29). Bai X; Yang Z; Zhu M; Dong B; Zhou L; Zhang G; Wang J; Wang Y Design and Synthesis of Potent HIV-1 Protease Inhibitors with (S)-Tetrahydrofuran-Tertiary Amine-Acetamide as P2–Ligand: Structure–Activity Studies and Biological Evaluation. *Eur. J. Med. Chem* 2017, 137, 30–44. [PubMed: 28554091]
- (30). Yang Z-H; Bai X-G; Zhou L; Wang J-X; Liu H-T; Wang Y-C Synthesis and Biological Evaluation of Novel HIV-1 Protease Inhibitors Using Tertiary Amine as P2-Ligands. *Bioorg. Med. Chem. Lett* 2015, 25, 1880–1883. [PubMed: 25838144]
- (31). Yan J; Huang N; Li S; Yang L-M; Xing W; Zheng Y-T; Hu Y Synthesis and Biological Evaluation of Novel Amprenavir-Based P1-Substituted Bi-Aryl Derivatives as Ultra-Potent HIV-1 Protease Inhibitors. *Bioorg. Med. Chem. Lett* 2012, 22, 1976–1979. [PubMed: 22306123]
- (32). Bungard CJ; Williams PD; Ballard JE; Bennett DJ; Beaulieu C; Bahnck-Teets C; Carroll SS; Chang RK; Dubost DC; Fay JF; Diamond TL; Greshock TJ; Hao L; Holloway MK; Felock PJ; Gesell JJ; Su H-P; Manikowski JJ; McKay DJ; Miller M; Min X; Molinaro C; Moradei OM;



- Nantermet PG; Nadeau C; Sanchez RI; Satyanarayana T; Shipe WD; Singh SK; Truong VL; Vijayasaradhi S; Wiscount CM; Vacca JP; Crane SN; McCauley JA Discovery of MK-8718, an HIV Protease Inhibitor Containing a Novel Morpholine Aspartate Binding Group. *ACS Med. Chem. Lett* 2016, 7, 702–707. [PubMed: 27437081]
- (33). Bungard CJ; Williams PD; Schulz J; Wiscount CM; Holloway MK; Loughran HM; Manikowski JJ; Su H-P; Bennett DJ; Chang L; Chu X-J; Crespo A; Dwyer MP; Keertikar K; Morriello GJ; Stamford AW; Waddell ST; Zhong B; Hu B; Ji T; Diamond TL; Bahnck-Teets C; Carroll SS; Fay JF; Min X; Morris W; Ballard JE; Miller MD; McCauley JA Design and Synthesis of Piperazine Sulfonamide Cores Leading to Highly Potent HIV-1 Protease Inhibitors. *ACS Med. Chem. Lett* 2017, 8, 1292–1297. [PubMed: 29259750]
- (34). Kolb HC; VanNieuwenhze MS; Sharpless KB Catalytic Asymmetric Dihydroxylation. *Chem. Rev* 1994, 94, 2483–2547.
- (35). Jacobsen EN; Marko I; Mungall WS; Schroeder G; Sharpless KB Asymmetric Dihydroxylation via Ligand-accelerated Catalysis. *J. Am. Chem. Soc* 1988, 110, 1968–1970.
- (36). Riva R; Banfi L; Danieli B; Guanti G; Lesma G; Palmisano G Indole Alkaloids. Enantioselective Synthesis of (–)-Alloyohimbane by a Chemoenzymatic Approach. *J. Chem. Soc., Chem. Commun* 1987, 1987, 299–300.
- (37). (a) Danieli B; Lesma G; Mauro M; Palmisano G; Passarella D First Enantioselective Synthesis of (–)-Akagerine by a Chemoenzymatic Approach. *J. Org. Chem* 1995, 60, 2506–2513. (b) Adams GL; Carroll PJ; Smith AB III Total Synthesis of (+)-Scholarisine A. *J. Am. Chem. Soc* 2012, 134, 4037–4040. [PubMed: 22280070] (c) Ghosh AK; Sarkar A Enantioselective Syntheses of (–)-Alloyohimbane and (–)-Yohimbane by an Efficient Enzymatic Desymmetrization Process. *Eur. J. Org. Chem* 2016, 2016, 6001–6009.
- (38). Dihydroxylation of 12 with OsO<sub>4</sub> and NMO resulted in diols 13 and 14 in 1:3 ratio.
- (39). Von Langen DJ; Tolman RL Resolution and Stereo-selective Synthesis of the Herpes Thymidine Kinase Inhibitor L-653180. *Tetrahedron: Asymmetry* 1997, 8, 677–681.
- (40). Toth MV; Marshall GR A Simple, Continuous Fluorometric Assay for HIV Protease. *Int. J. Pept. Protein Res* 1990, 36, 544–550. [PubMed: 2090647]
- (41). Koh Y; Amano M; Towata T; Danish M; Leshchenko-Yashchuk S; Das D; Nakayama M; Tojo Y; Ghosh AK; Mitsuya H In Vitro Selection of Highly Darunavir-Resistant and Replication-Competent HIV-1 Variants by Using a Mixture of Clinical HIV-1 Isolates Resistant to Multiple Conventional Protease Inhibitors. *J. Virol* 2010, 84, 11961–11969. [PubMed: 20810732]
- (42). Aoki M; Danish ML; Aoki-Ogata H; Amano M; Ide K; Das D; Koh Y; Mitsuya H Loss of the Protease Dimerization Inhibition Activity of Tipranavir (TPV) and Its Association with the Acquisition of Resistance to TPV by HIV-1. *J. Virol* 2012, 86, 13384–13396. [PubMed: 23015723]
- (43). For details of X-ray studies, please see Supporting Information.
- (44). Wlodawer A; Vondrasek J Inhibitors of HIV-1 Protease: A Major Success of Structure-assisted Drug Design. *Annu. Rev. Biophys. Biomol. Struct* 1998, 27, 249–284. [PubMed: 9646869]
- (45). Agniswamy J; Kneller DW; Brothers R; Wang Y-F; Harrison RW; Weber IT Highly Drug-Resistant HIV-1 Protease Mutant PRS17 Shows Enhanced Binding to Substrate Analogues. *ACS Omega* 2019, 4, 8707–8719. [PubMed: 31172041]
- (46). Otwinowski Z; Minor W Processing of X-ray Diffraction Data Collected in Oscillation Mode In *Methods in Enzymology, 276: Macromolecular Crystallography, Part A.*; Carter CW Jr., Sweet RM, Eds.; Academic Press: New York, 1997; pp 307–326.
- (47). McCoy AJ; Grosse-Kunstleve RW; Adams PD; Winn MD; Storoni LC; Read RJ; Phaser Crystallographic Software. *Phasercrystallographic software. J. Appl. Crystallogr* 2007, 40, 658–674. [PubMed: 19461840]
- (48). Winn MD; Ballard CC; Cowtan KD; Dodson EJ; Emsley P; Evans PR; Keegan RM; Krissinel EB; Leslie AGW; McCoy A; McNicholas SJ; Murshudov GN; Pannu NS; Potterton EA; Powell HR; Read RJ; Vagin A; Wilson KS Overview of the CCP4 Suite and Current Developments. *Acta Crystallogr., Sect. D: Biol. Crystallogr* 2011, 67, 235–242. [PubMed: 21460441]

- (49). Collaborative Computational Project, Number 4. The CCP4 Suite: Programs for Protein Crystallography. *Acta Crystallogr., Sect. D: Biol. Crystallogr* 1994, 50, 760–763. [PubMed: 15299374]
- (50). Potterton E; Briggs P; Turkenburg M; Dodson E A Graphical User Interface to the CCP4 Program Suite. *Acta Crystallogr., Sect. D: Biol. Crystallogr* 2003, 59, 1131–1137. [PubMed: 12832755]
- (51). Shen C-H; Wang Y-F; Kovalevsky AY; Harrison RW; Weber IT Amprenavir Complexes with HIV-1 Protease and its Drug-Resistant Mutants Altering Hydrophobic Clusters. *FEBS J.* 2010, 277, 3699–3714. [PubMed: 20695887]
- (52). Sheldrick GM Short History of SHELX. *Acta Crystallogr., Sect. A: Found. Crystallogr* 2008, 64, 112–122.
- (53). Sheldrick GM Crystal Structure Refinement with SHELXL. *Acta Crystallogr.* 2015, 71, 3–8.
- (54). Murshudov GN; Vagin AA; Dodson EJ Refinement of Macromolecular Structures by the Maximum-likelihood Method. *Acta Crystallogr., Sect. D: Biol. Crystallogr* 1997, 53, 240–255. [PubMed: 15299926]
- (55). Schüttelkopf AW; van Aalten DMF PRODRG: a Tool for High-Throughput Crystallography of Protein–Ligand Complexes. *Acta Crystallogr., Sect. D: Biol. Crystallogr* 2004, 60, 1355–1363. [PubMed: 15272157]
- (56). Lebedev AA; Young P; Isupov MN; Moroz OV; Vagin AA; Murshudov GN Ligand: A Graphical Tool for the CCP4 Template-restraint Library. *Acta Crystallogr., Sect. D: Biol. Crystallogr* 2012, 68, 431–440. [PubMed: 22505263]
- (57). Emsley P; Lohkamp B; Scott WG; Cowtan K Features and Development of Coot. *Acta Crystallogr., Sect. D: Biol. Crystallogr* 2010, 66, 486–501. [PubMed: 20383002]
- (58). Emsley P; Cowtan K Coot: Model-Building Tools for Molecular Graphics. *Acta Crystallogr., Sect. D: Biol. Crystallogr* 2004, 60, 2126–2132. [PubMed: 15572765]
- (59). Berman HM; Westbrook J; Feng Z; Gilliland G; Bhat TN; Weissig H; Shindyalov IN; Bourne PE The Protein Data Bank. *Nucleic Acids Res.* 2000, 28, 235–242. [PubMed: 10592235]

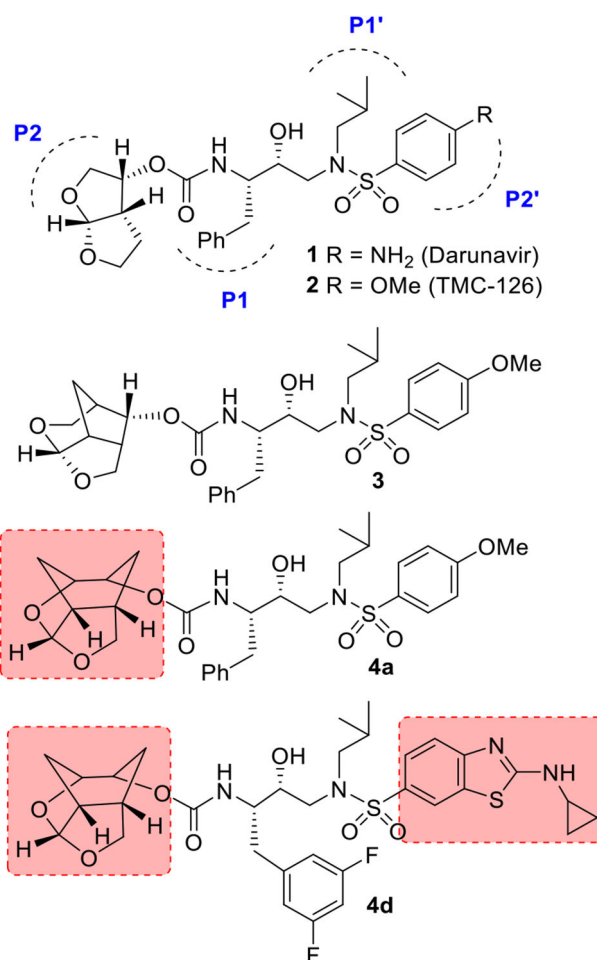


**Figure 1.**  
Structures of HIV-1 PIs 1–4.

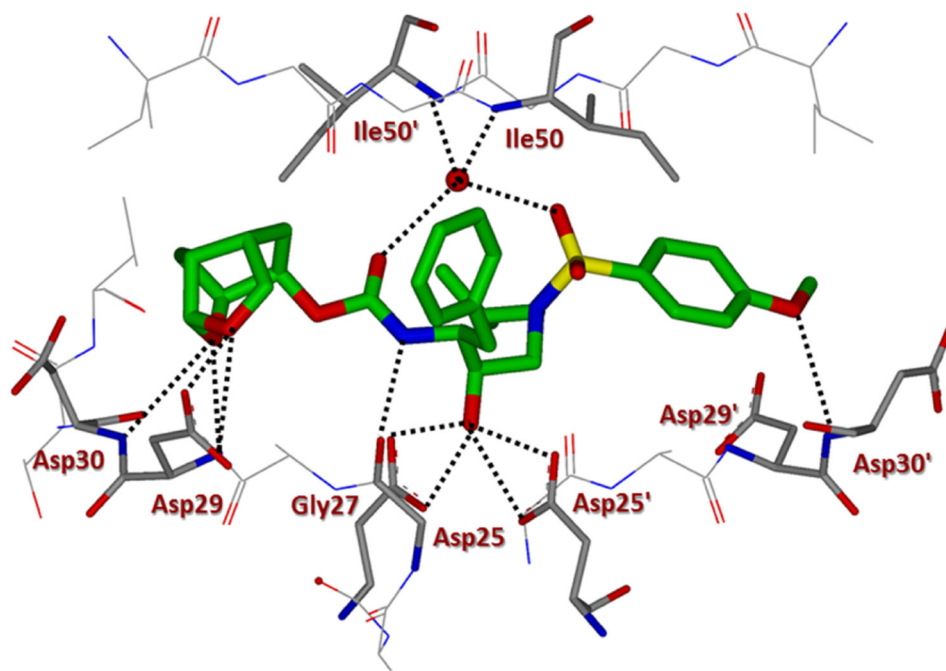


**Figure 2.** Inhibitor **4a**-bound HIV-1 protease X-ray structure is shown (pdb code: 6VOD). The inhibitor carbon atoms are shown in green and hydrogen bonds are shown by black dotted lines.

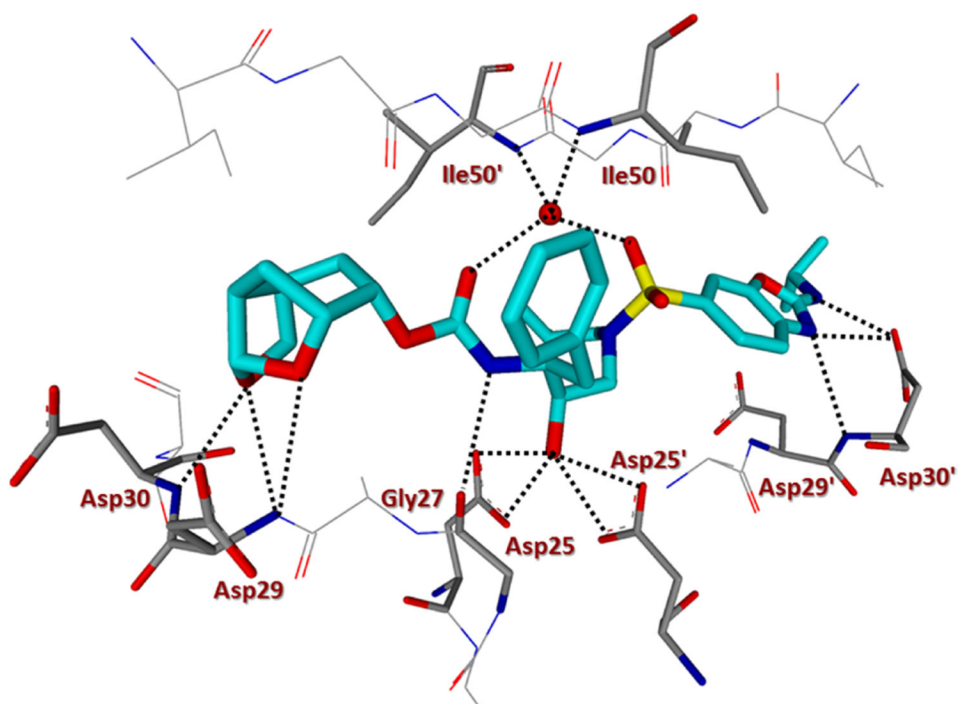


**Figure 3.** Inhibitor **5c**-bound HIV-1 protease X-ray structure is shown (pdb code: 6VOE). The inhibitor carbon atoms are shown in cyan and hydrogen bonds are shown by black dotted lines.

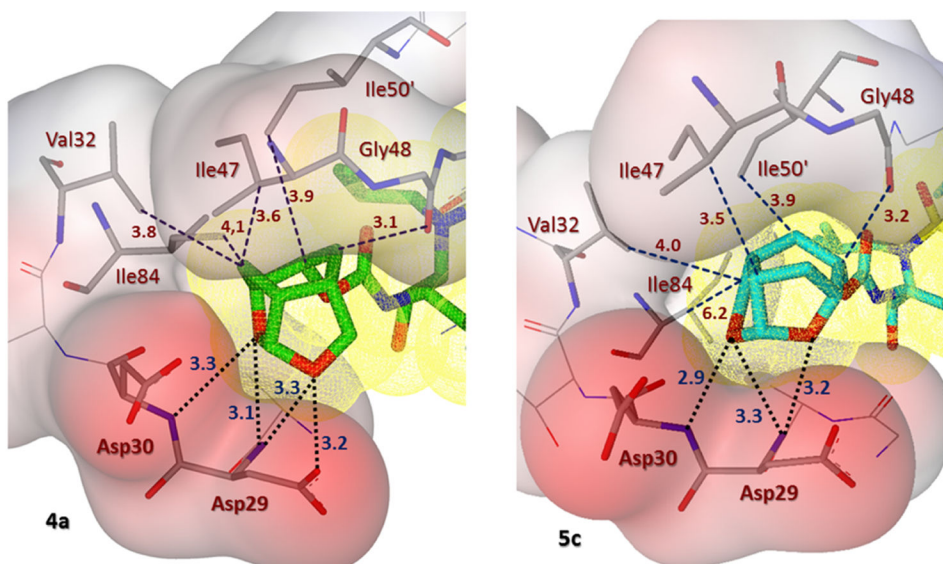
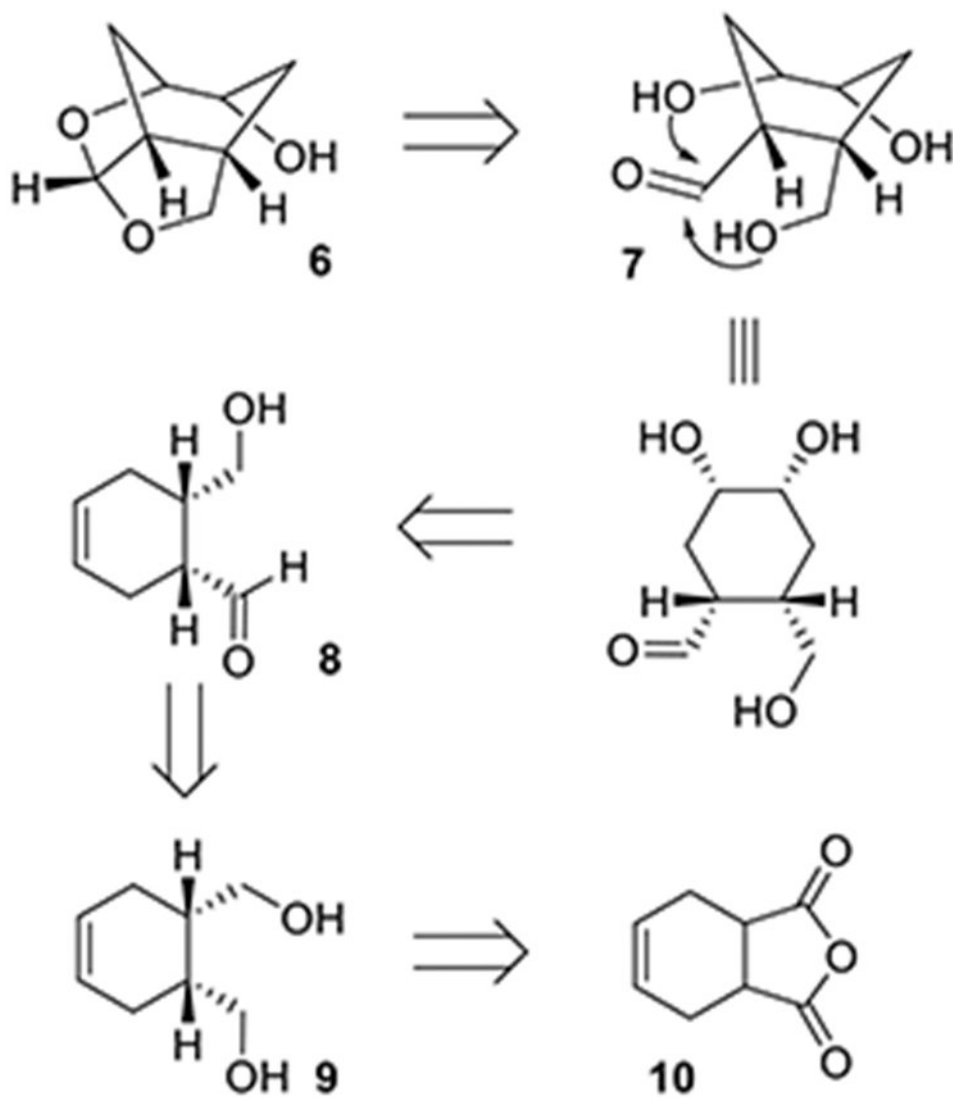
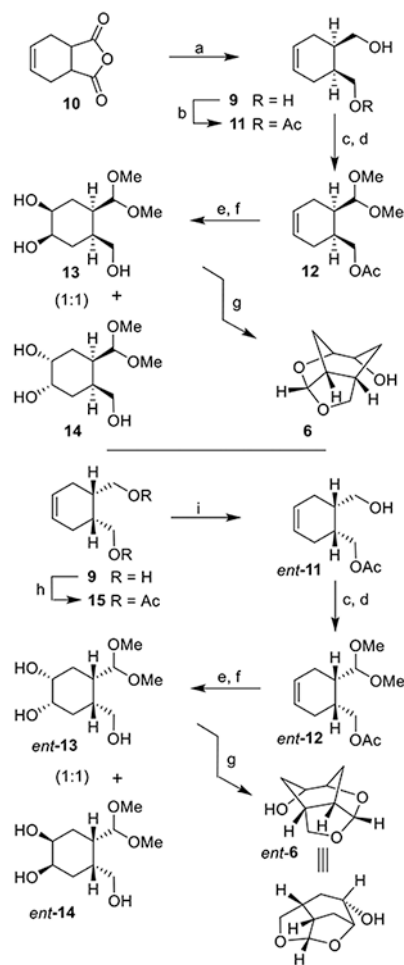


**Figure 4.** Side by side comparison of the new *Chf*-THF moiety of inhibitor **4a** (left, green carbon atoms) with the enantiomeric *Chf*-THF moiety of inhibitor **5c** (right, cyan carbon chain) inside the S2 subpocket. Both ligands form extensive van der Waals interactions (Val32, Ile47, Ile50', and Ile84 for **4a** and Val32, Ile47, and Ile50' for **5c**) in the S2 subsite. Also, they are located close to the periphery of the protease active site and form three strong hydrogen bonds in a similar fashion (black dotted lines).





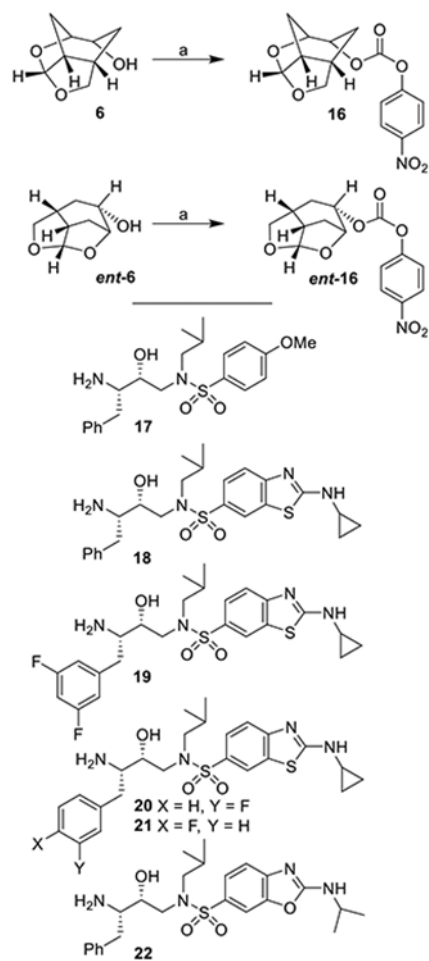
**Scheme 1.**  
Synthetic Strategy for the Cyclohexane-Fused *bis*-THF P2 Ligand Structure



**Scheme 2.**

Synthesis of Substituted Tricyclic P2 Ligands **6** and *ent-6*<sup>a</sup>

<sup>a</sup>Reagents and conditions. (a) LiAlH<sub>4</sub>, THF, 0 °C, 3 h (85%); (b) PPL, EtOAc, 23 °C, 12 h (82%); (c) (COCl)<sub>2</sub>, DMSO, TEA, CH<sub>2</sub>Cl<sub>2</sub>, -78 to 0 °C, 1.5 h; (d) CH(OMe)<sub>3</sub>, TBABr<sub>3</sub>, MeOH, 23 °C, 8 h (76% over 2-steps for **12**; 80% over 2-steps for *ent-12*); (e) AD mix-β, CH<sub>3</sub>SO<sub>2</sub>NH<sub>2</sub>, *t*-BuOH/H<sub>2</sub>O (1:1), 0–23 °C; (f) 1 N NaOH, MeOH, 0–23 °C, 3 h (90% over 2-steps for **13** & **14**; 88% over 2-steps for *ent-13* & *ent-14*); (g) CSA, CH<sub>2</sub>Cl<sub>2</sub>, 0 °C, 1 h (82% for **6** and 79% for *ent-6*); (h) Ac<sub>2</sub>O, Py, DMAP, CH<sub>2</sub>Cl<sub>2</sub>, 0–23 °C (98%); (i) PPL, 0.1 M phosphate buffer pH 7, 1 N NaHCO<sub>3</sub>, 23 °C, 16 h (84%).

**Scheme 3.**Synthesis of Activated Carbonates **16** and *ent-16*<sup>a</sup><sup>a</sup>Reagents and Conditions. (a) 4-NO<sub>2</sub>PhOCOCl, Py, CH<sub>2</sub>Cl<sub>2</sub>, 0–23 °C, 8 h (87% for **16** and 88% for *ent-16*)

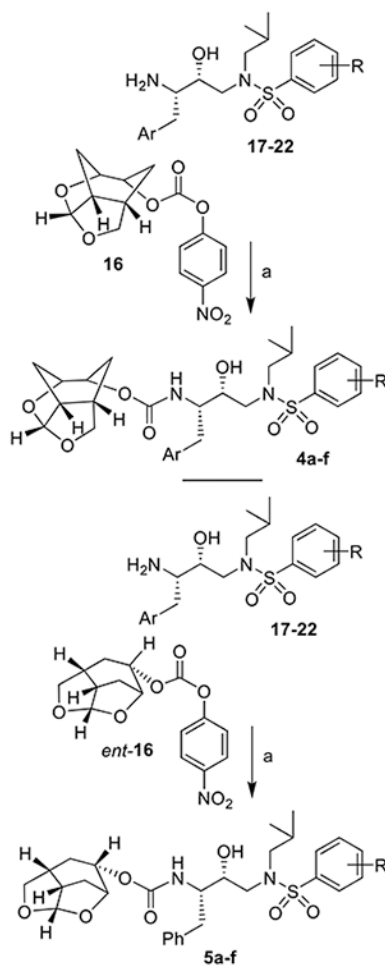
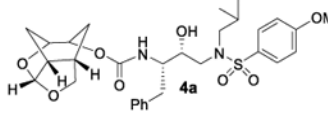
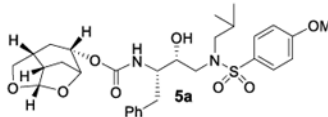
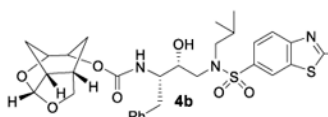
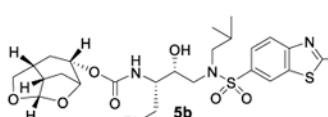
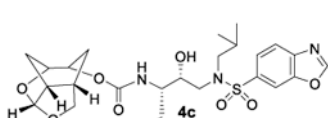
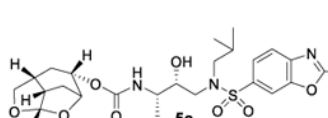
**Scheme 4.**Synthesis of PIs 4a–4f and 5a–f<sup>a</sup><sup>a</sup>Reagents and Conditions. (a) DIPEA, CH<sub>3</sub>CN, 23 °C, (59–87%)

Table 1.

HIV-1 Protease Inhibitory and Antiviral Activity of PIs

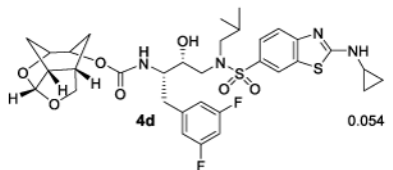
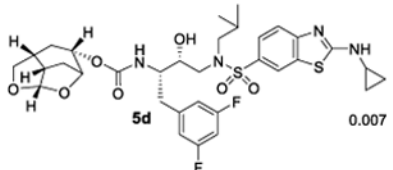
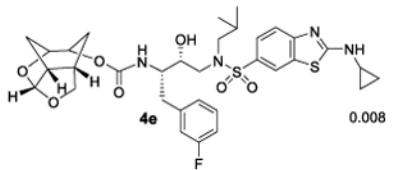
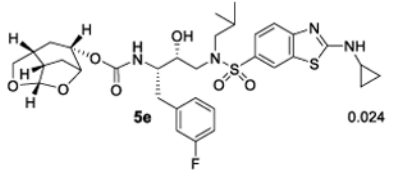
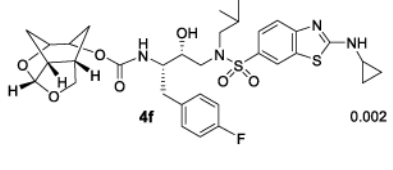
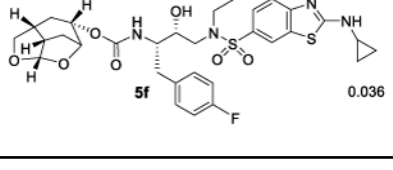
Entry	Inhibitor	$K_i$ (nM) <sup>a</sup>	$IC_{50}$ (nM) <sup>b</sup>
1.		0.008	38
2.		0.034	71.7
3.		0.002	3.3
4.		0.027	1.86
5.		0.006	1.73
6.		0.047	0.30

<sup>a</sup>  $K_i$  values represents at least four data points. Standard error in all cases was less than 7%. Darunavir exhibited  $K_i$  = 16 pM.

<sup>b</sup> Values are means of at least three experiments. Standard error in all cases was less than 5%. Darunavir exhibited antiviral  $IC_{50}$  = 3.2 nM, saquinavir  $IC_{50}$  = 21 nM.

Table 2.

## HIV-1 Protease Inhibitory and Antiviral Activity of PIs

Entry	Inhibitor	$K_i$ (nM) <sup>a</sup>	$IC_{50}$ (nM) <sup>b</sup>
1.	 <b>4d</b>	0.054	0.086
2.	 <b>5d</b>	0.007	2.25
3.	 <b>4e</b>	0.008	1.28
4.	 <b>5e</b>	0.024	2.7
5.	 <b>4f</b>	0.002	0.46
6.	 <b>5f</b>	0.036	0.4

<sup>a</sup>  $K_i$  values represents at least four data points. Standard error in all cases was less than 7%. Darunavir exhibited  $K_i$  = 16 pM.

<sup>b</sup> Values are means of at least three experiments. Standard error in all cases was less than 5%. Darunavir exhibited antiviral  $IC_{50}$  = 3.2 nM, saquinavir  $IC_{50}$  = 21 nM.



Table 3.

Antiviral Activity of 5c and 4d and Other PIs against Highly PI-Resistant HIV-1 Variants<sup>a, b, c</sup>

virus species	mean IC <sub>50</sub> in nM ± SD (fold-change)			
	ATV	DRV	compound 5c	compound 4d
wild-type	4.0 ± 0.7	4.2 ± 0.9	38 ± 1	0.034 ± 0.026
<i>in vitro</i> HIV-1 <sub>PR</sub> <sup>R</sup>	>1000 (>250)	26 ± 6(6.1)	350 ± 30 (9.1)	0.21 ± 0.07 (6.3)
HIV-1 <sub>ATV-5</sub> μM	430 ± 10 (107)	360 ± 50 (86)	>1000 (>26)	4.3 ± 0.2 (127)
HIV-1 <sub>DRV<sup>R</sup>P30</sub>	>1000 (>250)	370 ± 120 (89)	640 ± 510 (17)	4.5 ± 2.5 (133)

<sup>a</sup>The amino acid substitutions identified in protease of HIV-1<sub>ATV-5</sub> μM, HIV-1<sub>LPV-5</sub> μM, and HIV-1<sub>DRV<sup>R</sup>P30</sub> compared to the wild-type HIV-1<sub>NL4-3</sub> include L23I/E34Q/K43I/M46I/I50L/G51A/L63P/A71V/V82A/T91A, L10F/V32I/M46I/I47A/A71V/I84V, and L10I/I15V/K20R/L24I/V32I/M36I/M46L/L63P/K70Q/V82A/I84V/L89M, respectively.

<sup>b</sup>*In vitro* HIV-1<sub>PR</sub><sup>R</sup>, *in vitro* PI-selected HIV-1 variants.

<sup>c</sup>The EC<sub>50</sub> (50% effective concentration) values were determined by using MT-4 cells as target cells. MT-4 cells (10<sup>5</sup>/mL) were exposed to 100 TCID<sub>50</sub>s of each HIV-1, and the inhibition of p24 Gag protein production by each drug was used as an endpoint. Numbers in parentheses represent fold changes in IC<sub>50</sub>s for each isolate compared to the IC<sub>50</sub>s for wild-type HIV-1<sub>NL4-3</sub>. All assays were conducted in duplicate, and the data shown represent mean values (±1 standard deviation) derived from the results of two independent experiments.